AN ABSTRACT OF THE THESIS OF

Stephen John Calkins for the degree of Master of Science in Sustainable Forest Management presented on July 24, 2020.

Title: Transformation of Western Hemlock Tree Crowns by Dwarf Mistletoe

Abstract approved:

_____

David C. Shaw

Hemlock dwarf mistletoe (*Arceuthobium tsugense* subsp. *tsugense)* is an arboreal, hemiparasitic plant that principally parasitizes western hemlock (*Tsuga heterophylla*). Hemlock dwarf mistletoe exerts a profound influence on infected trees that can drastically change the structure of the tree crown due to reduced growth, top dieback, branch deformation and death, resulting in unique habitat structures, changed fire dynamics, and more severe drought impacts. Although dwarf mistletoe is important to tree crowns, most research has been from the ground or by felling trees. In this study, we climbed 16 western hemlock trees (age 97 – 321 years) across a gradient of infection (0 – 100% of branches infected) and measured occurrence of all dwarf mistletoe infections, branch and crown architecture, and dwarf mistletoe caused deformities. Sapwood area was measured at the top of buttressing or 1.37 m above the ground (*f*-diameter) and at base of live crown. To explore the impacts of increasing infection severity, over 25 different response variables were examined using linear and generalized linear models to estimate mean responses among the 16 western hemlocks. We developed three metrics of

severity as explanatory variables for the models: total infection incidence, proportion of all live branches infected, and proportion of all live, infected branches with 33 percent or more foliage distal to infection. Many effects of dwarf mistletoe on crown structure appear subtle, except for deformations. Increasing severity led to crowns experiencing an apparent compaction, where crown volume was reduced while deformity volume increased, and crown volumes became increasingly comprised of deformities. A strong effect of dwarf mistletoe intensification is the reduction of branch foliage and an increase in the proportional amount of foliage distal to infections, and therefore a likely reduction in carbohydrates available to tree growth. Sapwood areas at *f*-diameter and at base of live crown were unrelated to all metrics of infection severity. Branch length and diameters were also unaffected by increasing infection severity despite heavily infected branches supporting 1 to 70 infections. This suggests infected trees compensate for the water and nutrient loss through changes to the crown architecture such as reduced foliage instead of through conductive tissues. Our results suggest shifts in crown structure reflect a shift in function, from prioritizing biomass production and growth, to tree survival.

Transformation of Western Hemlock Tree Crowns by Dwarf Mistletoe

by
Stephen John Calkins

A THESIS

submitted to

Oregon State University

in partial fulfillment of
the requirements for the
degree of

Master of Science

Presented July 24, 2020
Commencement June 2021

Master of Science thesis of Stephen John Calkins presented on July 24, 2020.

APPROVED:

_____

Major Professor, representing Sustainable Forest Management

_____

Head of the Department of Forest Engineering, Resources, and Management

_____

Dean of the Graduate School

I understand that my thesis will become part of the permanent collection of Oregon State University libraries. My signature below authorizes release of my thesis to any reader upon request.

_____

Stephen John Calkins, Author

ACKNOWLEDGEMENTS

I am enormously grateful to many people, whose contributions, big and small, have made this research project a reality and enriched my life in numerous ways. I am thankful for the guidance, support, and ever-present belief in me and this work from my advisor, Dave Shaw. From our first conversation, he has been a source of constant enthusiasm and always treated me and those around him with respect and kindness. Working with him has given me a newfound appreciation for all the things that shape our forests, especially for those little engineers of the canopy.

I am blessed to be in such a supportive community of tree climbers, without whom I could never have completed this project. Sky Lan devoted an entire summer to helping me collect data in the trees. She was never afraid of challenging work or long days and her knowledge and experience shaped my field work and this project. Russell Kramer has provided inspiration, guidance, and a git'er done attitude I could count on throughout this whole research project. Russell first taught me to climb trees which opened my eyes to life above ground, and for that I owe him a great deal.

I am sincerely grateful for Mik Miazio, Elena Lauterbach, Kasey Swenson, Richard Tarkington, Madison Stone, Preston Durham, Russell Kramer, Jessica Jemison, Amanda Brackett, Matthew Aghai, Ryan Keeling, Brian French, Jimmy Swingle, Stan Pennors, Adam Sibley, Hannah Prather, Claire Brase, and Mark Schulze for all your help rigging, climbing, and measuring these trees, without which, this research would have never been completed. Eric Forsman and Jimmy Swingle are tree climbing gurus and I

am fortunate to have received training and guidance from them early on. Katie Nicolato captured the climbing blitz with excellent drone photography and footage and is a stellar video editor.

Rob Pabst, Gabi Ritokova, and Andy Bluhm were a constant source of support and inspiration. From my first day, they made me feel welcomed and were always happy to share a conversation with me. I also appreciate the support of my committee members, Julia Jones, Dave Bell, Matt Powers, and Glenn Howe. Ariel Muldoon provided invaluable guidance from experimental design to statistical analysis and interpretation, and always had a patient answer for my many questions. Henry Lee and McKenzie Vogel generously gave us their time to cross-date our cores and thanks to Henry I will never look at time series data the same way again.

Matt Barker and Sylvan Pritchett helped me stay sane through many days and nights spent in the computer lab. Adam Sibley was the source of many enriching conversations and adventures. Whether in the trees or on the ground, they gave me something to look forward to when times were toughest, and I am thankful for their support and friendship.

Thank you to the HJ Andrews Experimental Forest and LTER network for allowing us to climb trees there, providing lodging, and help with field season logistics. This work was supported by funding from the College of Forestry Graduate Fellowship at Oregon State University.

TABLE OF CONTENTS

TABLE OF CONTENTS (Continued)

LIST OF FIGURES

LIST OF TABLES

Transformation of Western Hemlock Tree Crowns by Dwarf Mistletoe

CHAPTER 1 -- INTRODUCTION

Background

In the Pacific Northwest, from B.C. to northern Oregon, west of the Cascades, forest land is dominated by the western hemlock (*Tsuga heterophylla*) cover type (Franklin and Dyrness, 1973). These forests contain a suite of coniferous species, a few belonging to the largest and longest-lived tree species in the world, such as Douglas-fir (*Pseudotsuga menziesii*), western red-cedar (*Thuja plicata*), and Sitka spruce (*Picea sitchensis*) (Franklin and Dyrness, 1973). The development of Douglas-fir/western hemlock forests is described in Franklin et al. (2002) as occurring through eight stages: disturbance/legacy creation; cohort establishment; canopy closure; biomass accumulation/competitive exclusion; maturation; vertical diversification; horizontal diversification; pioneer cohort loss. Although this process likely does not occur linearly through time (Reilly and Spies, 2015). Disturbance and legacy creation processes result in exposed mineral soil and a high light environment, ideal for Douglas-fir establishment and growth. After establishment, Douglas-fir dominates the overstory through the maturation stage, where shade tolerant species such as western hemlock grow into intermediate and co-dominant positions in the canopy, sometimes taking 250 – 300 years. Eventual loss of Douglas-fir in the overstory may take 800 to 1000 years and without disturbance, these old growth forests transition into stands dominated by western

hemlock and western red-cedar (or another shade tolerant conifer) (Waring and Franklin, 1979).

In these forests and globally, large, old trees are one of the key features providing structure essential for promoting productivity, maintaining micro-habitats, enhancing biodiversity, and sequestering carbon (Carey and Wilson, 2001; Ishii et al., 2004; Lutz et al., 2018; Michel and Winter, 2009; Shaw et al., 2004; Sillett et al., 2010), and are important considerations for achieving non-timber, management objectives (Franklin et al., 2002). Old trees develop their crowns through a multitude of abiotic and biotic factors that make them unique from young and mature forests (Sillett et al., 2010; Winter et al., 2002). In recent decades, the emphasis on understanding the canopy structure of these incredible trees and forests has produced many studies attempting to quantify structural aspects of the canopy (Ishii et al., 2017; Kramer et al., 2018; Van Pelt et al., 2004; Van Pelt and Sillett, 2008) and an installation of a canopy crane (Shaw and Greene, 2003). However, most of this work focuses on the largest trees and surprisingly little work has been devoted to the canopy structure of western hemlock.

Van Pelt and Nadkarni (2004) showed that in stands up to 250 years old, western hemlock made up a marginal amount of total canopy cover. As the stands increased in age however, hemlock contributed a substantial portion of the total canopy cover. In older sampled stands of 500 and 650 years, western hemlock made up 59 and 34% of canopy cover, respectively. In the oldest sampled site (~950 years) western hemlock made up about 43% of the canopy cover and Pacific silver fir (*Abies amabilis*) made up 53%, while only one living Douglas-fir remained. Western hemlock contributes

significantly to the structure and volume of old growth forest and in younger, naturally regenerated stands, western hemlock most likely constitutes much of the suppressed and intermediate trees.

Old growth forests host a wide variety of tree pathogens above and below ground that contribute to the process of complex canopy structure formation (Castello et al., 1995; Hansen and Goheen, 2000). Prominently, western hemlock dwarf mistletoe (*Arceuthobium tsugense* subsp. *tsugense*), infects the crowns of western hemlocks resulting in unique structural features (Hawksworth and Wiens, 1996). In Oregon, 10.8% of all western hemlocks are infected with dwarf mistletoe, with 7% being moderately or severely infected (Dunham, 2008). Dwarf mistletoes create habitat features, affects fuel structures, and changes forest structure overall (Muir and Hennon, 2007). The Johnson's hairstreak butterfly (*Callophrys johnsoni*) relies on the aerial shoots for food, while the northern spotted owl (*Strix occidentalis caurin*a) and marbled murrelet (*Brachyramphus marmoratus*) use the witches' brooms and swollen branches for nesting platforms, caused by infection (Davis, 2010; Forsman et al., 1984). Numerous rodent nests can be found in branches with the largest and most developed witches' brooms. Severe dwarf mistletoe infections accelerate mortality in western hemlocks resulting in an increased abundance of snags and dead wood in canopies important for cavity nesting birds (Shaw et al., 2004). Accumulation of fuels in witches' brooms and lowering of fuels to the forest floor increase the susceptibility of these forests to stand replacing fire (Shaw et al., 2004). These alterations to fuels and structure may also influence fire at the local level to shape fire refugia (Shaw and Agne, 2017).

Figure 1. A mix of uninfected to severely infected western hemlocks in an old growth forest at the H.J. Andrews Experimental Forest, OR, US. Uninfected or lightly infected trees in the right-hand background next to heavily infected trees (arrows indicate two heavily infected trees), with western hemlock mortality with heavy infection severity behind them.

Dwarf Mistletoe Biology and Significance

Dwarf mistletoe is spread by explosively discharged seed, produced from aerial shoots of the parasite which emerge from infected branches (Hawksworth and Wiens, 1996). Hemlock dwarf mistletoe plants are dioecious (Figure 2); each individual infection may be male or female (Hawksworth and Wiens, 1996). Seeds are coated in a sticky

substance called viscin that lets the seed slide down needles and branches when wet. Germination is most successful when the seed slides down the needles and encounters the needle-branch connection, especially on young, thin-barked branches (Muir and Hennon, 2007). Dwarf mistletoe seeds contain chlorophyll in the endosperm allowing photosynthesis (Hawksworth and Wiens, 1996). Once germination starts, a small growth is produced that mechanically pushes into the branch's cortex. A root-like structure called the haustorium then develops. Once the haustorium encounters the cambium of the branch, runners grow in the cambium and sinkers develop in the sapwood, not by ramification in the wood, but by the sapwood growing around the wood as the branch responds to infection. The combined cambium and xylem colonization of the dwarf mistletoe, allows water and nutrients to be absorbed from the host branch (Hawksworth and Wiens, 1996). Shaw and Weiss (2000) found aerial shoots to be skewed to high light environments within the canopy and that height and light are highly correlated in the canopy.

Figure 2. Aerial shoots of two different dwarf mistletoe infections. Left: A female plant with developed seeds close to ejection. Right: A male plant fully opened flowers. These are large plants, found at the tops of two infected trees.

When dwarf mistletoe intensifies within a western hemlock crown, the morphology of the tree can change drastically. During the first years of infection, the host branch produces a swollen ring of sapwood at the site of infection (Muir and Hennon, 2007). Foliage area and fine branches increase exponentially forming bushy, characteristic, deformations in branch form commonly called “witches’ brooms” (Figure 3). These witches’ brooms contain dense growths of fine branches and leaves layered horizontally that can serve as a platform-like structure. Hawksworth & Wiens (1996) suggest formation of deformations are caused by altered levels of hormones, namely cytokinins, which was supported by Logan et al.’s (2013) findings in infected white spruce. In advanced stages of infection, branches swell to massive sizes. Infections to the leader or upper branches of a tree result in a flat broom top where no other branches take over as leader which severely limits or stops height growth (Muir and Hennon, 2007). Bole infections may also occur, but this is usually the result of leader infections of young hemlocks and are not commonly observed at the tops of older trees. Branch dieback, top death, and loss of foliage and photosynthetic capacity follow as infection severity increases (Figure 4). Impacts to growth of infected trees may change throughout time as infection severity increases. One study of infected western hemlocks in SW Washington, found that bole diameter growth increased as infection severity initially increased, but in the most severe infections, bole diameter growth greatly decreased (Marias et al., 2014). Deformities (witches’ brooms, swellings, etc.) are thought to develop and change as the infection ages and abiotic factors influence form of the branch. Once a branch is infected, dwarf mistletoe remains

for as long as the host tree is alive and may increase branch longevity, resulting in decades old (sometimes defoliated) infected branches (Muir and Hennon, 2007). Dwarf mistletoe has also been observed to increase the shade tolerance of branches: infected branches keep their foliage low in the crown often longer where uninfected branches persist (Muir and Hennon, 2007). A study found infection structures are skewed to the lower to mid positions in the canopy (Shaw et al., 2005). Infection can directly, or indirectly lead to tree death creating gaps in the canopy. These gaps provide the necessary light for understory plants to grow, increasing biodiversity of the forest (Franklin et al., 2002). These morphological changes to individual trees lead to forest wide structural changes in the canopy.

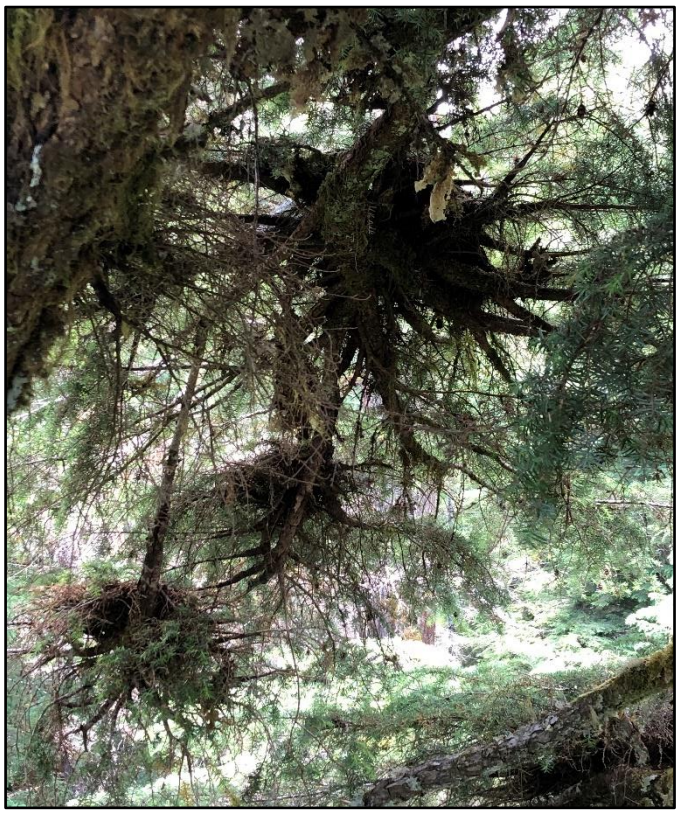

Figure 3. Three deformities that well represent the classic witches' broom. These have likely been infected for a long period of time based on their pronounced swellings and size. While hemlock dwarf mistletoe creates non-systemic infections, these deformities may contain several individual infections. Picture by Dave Shaw.

Carbon Accumulation and Growth Implications

In addition to their unique canopy structure, old growth trees in Pacific Northwest forests sequester amounts of carbon rarely matched by other trees into old age (Stephenson et al., 2014). In old trees, stem growth below the base of the live crown may stop or decline but stem growth above the base of the live crown continues (Ishii et al., 2017; Van Pelt and Sillett, 2008). Thus, old growth trees continue to increase their mass year-after-year (Sillett et al., 2010). Estimates of carbon accumulation are important for

climate change modeling. Dwarf mistletoe significantly changes the morphology of western hemlocks but also significantly changes the anatomical structure and physiological function of the host tree. Meinzer et al. (2004) found daily water use by infected trees is significantly less than in uninfected trees. Because of this, severely infected trees were estimated to reduce carbon accumulation by 60 percent. Estimates of carbon accumulation and biomass of old growth forests may be inaccurate if these effects are not considered.

Figure 4. A heavily infected western hemlock severely impacted by dwarf mistletoe. Dwarf mistletoe may increase the likelihood of branch mortality when infection severity

becomes too high and the tree is unable to meet its own respiratory needs while sustaining one to likely many dwarf mistletoe infections per branch. The dead top is another common symptom of high severity infection by dwarf mistletoe.

Estimates of biomass and productivity are commonly based on measurements taken from the ground such as DBH or height. However, in Sitka spruce, diameter-based measurements of biomass and productivity were less precise than those that included both diameter and sapwood area (Bormann, 1990). The addition of sapwood area represented observed differences in leaf area which accounted for differences observed in biomass. This relationship is an extension of the Pipe-Model theory: the cross-sectional area of sapwood at any height is related to the area (or dry mass) of foliage supported above that height (Shinozaki et al., 1964a, 1964b). A multitude of studies have been conducted examining this relationship across many species and climates, including western hemlock (Ewers and Zimmermann, 1984; Sattler and Comeau, 2016; Sellin and Kupper, 2006; Waring et al., 1982). These studies, however, are often based on young, healthy trees that can be easily felled. Dwarf mistletoe infections reduce the area and decrease the efficiency of western hemlock foliage and affect the water transport efficiency of infected branch xylem (Meinzer et al., 2004). It is important to understand how dwarf mistletoe changes western hemlock live branch proportion and the proportion of crown affected by infection and how this is related to bole sapwood area to produce accurate estimates of biomass and better understand infected trees' physiological impacts.

Management Implications

Forest managers need quantified measures of structural complexity to emulate disturbances and develop silvicultural prescriptions or accurately model stand development (Franklin et al., 2002; Reilly and Spies, 2015). A large literature base exists for managing dwarf mistletoe for a wide range of management objectives, summarized by Muir & Hennon (2007), that depend on the potential for spread and intensification of dwarf mistletoe. Currently, general impacts to infected western hemlocks are understood, however managers are unable to quantify canopy structure created by dwarf mistletoe. The dwarf mistletoe severity rating system primarily used to estimate impacts is the Hawksworth 6-Class Dwarf Mistletoe Rating (DMR) system (Hawksworth, 1977), adapted from open ponderosa pine (*Pinus ponderosa*) forests infected with another dwarf mistletoe, *A. vaginatum* subsp. *cryptopodum*. In the tall forests of the Pacific Northwest, treetop obscurity makes this system difficult to implement accurately. Shaw, Freeman, and Mathiasen (2000) found this system to be highly subjective and inconsistent when applied to old growth Douglas-fir/western hemlock forests of SW Washington State, US. Despite this, researchers have created growth models that predict spread and intensification of dwarf mistletoe using datasets based on this DMR system (Robinson and Geils, 2006; Trummer et al., 1998).

Future projections from modeling may not accurately reflect the true growth trajectory or development of mature and old growth forests without accurately measuring dwarf mistletoe infected western hemlock. For example, forest managers seeking to prescribe burn areas may need to incorporate dwarf mistletoe counts or measures of

severity to manage fire severity (Shaw and Agne, 2017). Dwarf mistletoe is thought to re-infect forested stands by surviving in fire refugia. Predicting how and where these refugia will form will be necessary for forest managers. Therefore, precise measurements of severity or incidence are important to reveal ongoing processes that have been overlooked by the coarse scale DMR, which are almost impossible to measure in old growth trees without accessing the crown.

Measuring *Tsuga heterophylla* Crowns

Climbing into western hemlock crowns, across an infection gradient of uninfected to completely infected (every branch has at least one infection), to completely map the tree crown along with measurements of sapwood area, can provide the necessary measurements to quantify estimates of growth impacts and link these to physiological impacts. Sole reliance on ground-based measurements is inaccurate for estimating mature and old tree stem, leaf, and branch growth; the best indicators of these growth attributes are measured in the crown, such as at the base of the live crown (Ishii et al., 2017). A comprehensive crown inventory with a variety of measurements of all infections and branches can elucidate if structural changes forest managers think are important for wildlife or fire are occurring in these trees and to what degree. Climbing also avoids inaccuracies from using the DMR system and allows a fine-scale measurement of infection severity. There has been a large amount of information published about the crown structure, growth and development, and biomass of Douglas-fir, coastal redwood (*Sequoia sempirvirens*), Sitka spruce, and *Eucalyptus regnans* that was produced by

accessing these trees' canopies (Kramer et al., 2018; Sillett et al., 2019, 2018; Van Pelt and Sillett, 2008). Canopy cranes have also been constructed for this type of work (Shaw and Greene, 2003). While incredibly effective for canopy studies, cranes require more resources to set up and operate and do not allow access to the near bole area. Most studies of infected *T. heterophylla* crowns have required tree felling compromising data quality or have put a focus on younger trees with more accessible crowns (Smith, 1969). Recent advances in tree climbing techniques allow the same detailed measurements of tree canopies with minimal impact to valuable, old trees (Anderson et al., 2020) and techniques commonly used for arboriculture can be transferred easily to large trees (Jepson, 2000). An important consideration for all tree climbing endeavors is safety: climbing trees with any amount of disease is dangerous work so an emphasis is placed on selecting safe trees to climb.

Research Question

How does western hemlock dwarf mistletoe affect the development and structure of the crown and sapwood area of western hemlock in mid-elevation forests in the Central Oregon Cascades?

Rationale and Significance

There are several reasons to investigate the structural changes dwarf mistletoe causes in western hemlocks. First, mature and old growth forests provide numerous ecological benefits that are unmatched by other forest types through development of

unique structure. Canopy structural components such as limb size and location, dead or deformed treetops, and canopy size all affect microclimate, carbon storage, and biodiversity (Parker et al., 2004; Sillett et al., 2010; Spies and Duncan, 2012). Dwarf mistletoe causes changes to each of these structural components in western hemlocks which means it has a direct effect on the biodiversity and ecological benefits of a forest.

Second, western hemlocks contribute a significant amount to biomass and canopy volume of mature and old growth forests. Old growth trees store amounts of carbon rarely matched by other forest types around the world and while the largest and oldest trees in these forests may play the biggest role, results show western hemlock plays a prominent role in forests and contributes much to the structure of the forest. Most of the recent canopy and biomass quantification work focuses on the largest trees such as coastal redwoods, Douglas-fir, Sitka spruce and *Eucalyptus regnans*. These forest giants, while impressive, are unfortunately not the majority of trees on the landscape and as such these detailed studies have a limited scope of applicability. Other research detailing anatomical or morphological changes have little or no mention of forest pathogens.

In trees infected with a pathogen such as dwarf mistletoe, changes in the leaf area and water and nutrient transport system occur. Therefore, estimates of the rate of carbon accumulation or biomass may be inaccurate. However, by measuring dwarf mistletoe's morphological changes to western hemlock, and incorporating the pipe-model theory, sapwood area measured at DBH may be a useful indicator for hydraulic architectural changes. This work will provide an important starting point for further investigation of western hemlock canopy structure and biomass and dwarf mistletoe's influence on it.

Third, there are management implications for producing accurate estimates of canopy structure. Complex canopy structure is important to consider for achieving management objectives such as wildlife habitat, fire control, and carbon sequestration. A growing field of forestry, referred to as ecological forestry, seeks to balance ecosystem services and forest products in a sustainable manner. An important part of this management style is emulating disturbances naturally found on the landscape with silvicutural prescriptions and as such, forest managers need accurate measures of structural complexity to inform their prescriptions. Also, most forest inventories are created using metrics easily measured from the ground. Some of these metrics such as live crown base height, are used to evaluate canopy structure from the ground and serve as proxies for what we know about tree crowns without needing foresters to climb trees. Even DBH, when used to estimate biomass, incorporates assumptions about tree canopies such as the wood anatomy above live crown base. Often these assumptions are created from destructively sampled trees that otherwise would have needed their canopies accessed. Lastly, fire seasons have become longer, and fires become uncharacteristically severe. Forest managers need to include measurements in their inventories for predicting fire risk and fuel loading. Dwarf mistletoe's role in increasing the likelihood of crown fires and requiring fire refugia to persist on a landscape need to be balanced by managers. The previously described relationship of DBH and changes to sapwood area may be useful for this as well.

Goals and Objectives

Goal

Assess the impacts of forest pathogens on forest structure using the western hemlock – western hemlock dwarf mistletoe, host – parasite interaction as a model pathological-system.

Objectives

Our objectives are to determine how:

1. The structure and morphology of the western hemlock tree crown change across an infection severity gradient at the branch and crown level.
2. The sapwood area of the western hemlock tree bole change across an infection severity gradient at *f*-diameter and at base of live crown and what implications this may have on physiological function.

CHAPTER 2 – MANUSCRIPT

Dwarf mistletoes (*Arceuthobium* spp., Viscaceae) are native, flowering, hemi-parasitic plants that can severely impact host structure and function (Glatzel and Geils, 2009; Hawksworth and Wiens, 1996). *Arceuthobium tsugense* subsp. *tsugense* infects the crowns of its primary host *Tsuga heterophylla* causing deformation to woody tissues and reductions to growth, total foliage, photosynthetic capacity and water use efficiency (Hawksworth and Wiens, 1996; Marias et al., 2014; Meinzer et al., 2004). The most severely infected trees often exhibit dead tops, an abundance of dead branches, and branches supporting several deformities and numerous infections (Muir and Hennon, 2007). The infection intensification process profoundly transforms the structure of the tree crown and forest canopies as plants increase in number and cause deformation.

There is a large volume of literature on *A. tsugense*, mostly focused on managing growth impacts or eliminating and limiting spread into uninfected, younger stands (Geils et al., 2002; Muir and Hennon, 2007; Parmeter, 1978). However, trends in the last several decades of forestry and silviculture have shifted to promoting structural complexity, a focus on resilience, and a recognition of large old trees (Fahey et al., 2018; Franklin et al., 2002; Lutz et al., 2018). Study of older, infected *T. heterophylla* uncovered the extent of impacts to growth and structure, and that these increase over time and severity, and increase susceptibility to abiotic stressors (Bell et al., 2020; Marias et al., 2014; Mathiasen et al., 2008; Meinzer et al., 2004). Ecological benefits derived from their unique structures such as increasing biodiversity and providing bird and mammal habitat

were recognized (Griebel et al., 2017; Shaw et al., 2004). Infected trees also play a prominent role shaping local fire severity (Shaw and Agne, 2017).

Crown mapping has proved insightful for tree species that create the largest individuals and commonly co-occur with *T. heterophylla* such as *Pseudotsuga menziesii*, *Sequoia sempirvirens*, and *Picea sitchensis* (Ishii et al., 2017; Kramer et al., 2018; Sillett et al., 2010; Van Pelt et al., 2004; Van Pelt and Sillett, 2008). Crown mapping produces a complete description of a tree's crown architecture and provides valuable data for analysis of crown components such as foliage and branch volumes. Previous crown mapping efforts have not targeted *T. heterophylla* infected with *A. tsugense* despite its contribution of unique canopy structures and volume across Northwest forests (Shaw et al., 2004; Van Pelt and Nadkarni, 2004). In Oregon it is estimated 10.8% of all *T. heterophylla* are infected with *A. tsugense* and that 7% of those are moderate or severe (Dunham, 2008). Crown architecture and volume impacts have been more easily studied in forests where tree crowns are more visible or accessible such as in *Pinus contorta* or *P. ponderosa* (Agne et al., 2014; Godfree et al., 2003, 2002; Hoffman et al., 2007). Although, these trees also lack comprehensive measurements of the crown's architectural transformation from dwarf mistletoe infection.

In this exploratory study we apply an adapted crown mapping process for the first time to 16 *T. heterophylla* crowns, across a gradient of infection severity (i.e., dwarf mistletoe rating) in mature and old-growth forests at the HJ Andrews Experimental Forest. The adaption will incorporate protocols for measuring the infection-induced deformities (Van Pelt et al., 2004). We assess the impacts to branch form and foliage,

crown architecture, and sapwood area due to infection through statistical models of crown mapped data and examine the role deformity class plays in the crown's architecture. Canopy mapping allowed us to use three fine-scale metrics of infection severity as explanatory variables: the proportion of all live branches that are infected (branch severity), the proportion of live branches with 33% or more foliage distal to infection (foliage severity), and the total number of individual infections or dwarf mistletoe plants (incidence). These took the place of the Hawksworth 6-class dwarf mistletoe rating system in our models as infection severity ratings (Hawksworth, 1977). Lastly, we connect our findings to previous work to bridge gaps between the physical alterations to tree form and its physiological and ecosystem function. We expected branches to have reduced foliage cover as a response to reported reductions in overall infected tree water use, as well as smaller lengths and diameters as infection severity increased. We expected to see a compensatory shift in sapwood associated with decreased foliage area and increasing infection severity. We also expected tree crown volumes to shrink as infection severity increased.

Materials and Methods

Study Site

This research was conducted at the HJ Andrews Long-Term Ecological Research (LTER) site and Experimental Forest (HJA), located in the western Cascade Mountains, northeast of the community of Blue River, McKenzie Bridge, Oregon (44.2°N, 122.2°W) and is part of the Willamette National Forest, administrated by the USFS PNW Research

station (https://andrewsforest.oregonstate.edu). Topographical features are representative of the western Cascade Range, with steep mountainous terrain, exposed ridges, sheltered valleys, and a high degree of topographic heterogeneity with elevations ranging from 410 to 1630 m. Topography and soils have been shaped by volcanic, glacial, fluvial, and other geomorphological processes (Zald et al., 2016). Low elevation soils are characterized by volcanic rock composed of mudflows, ash flows, and stream deposits, transitioning to mostly lava flows as elevation increases (Swanson and Jones, 2002).

Climatic conditions are typical of maritime climates: wet, mild winters and dry, cool summers. Mean temperatures range from 1° C in January to 18° C in July, varying with elevation, aspect, and topographical setting. Precipitation falls primarily from November to March, averaging 2300 mm yr^{-1} at low elevations to over 3550 mm yr^{-1} at higher elevations. In lower elevations, rain mixed with snow is common during winter and snowpack rarely persists. Snow is more common at higher elevations; above 1000 – 1200 m seasonal snowpack develops, about 1 m in depth.

The sampled trees stand in old and mature forests, below 1000 m in elevation in the Western Hemlock Vegetation Zone described by Franklin and Dyrness (1973) which comprise the forest community surrounding each tree. Large, old *Pseudotsuga menziesii* dominate the overstory but are spread sparsely throughout the forest. *Tsuga heterophylla* co-dominates in the overstory and *Thuja plicata* is present in the overstory on the wetter sites, in valley bottoms and stream-side. Other characteristics of old-growth such as multi-storied canopy structure and an abundance of dead wood are also common (Spies

and Franklin, 1991). Understory tree species included *T. heterophylla*, *T. plicata*, and *Taxus brevifolia*. Regenerating trees are almost entirely *T. heterophylla* due to the dense canopies. The most common understory species are *Polystichum munitum*, *Rhododendron macrophyllum*, *Mahonia aquifolium*, *Gaultheria shallon*, *Vaccinium parvifolium*, and *Acer circinatum*.

Forest establishment is due to a mix of wildfire and logging. High and mixed severity wildfire is the primary disturbance agent at HJA, with the oldest stands (>500 years old) established post high severity fire (Tepley et al., 2013). Non-stand replacing fires are also common resulting in complex forest structure (Tepley et al., 2013). Forest establishment and disturbance processes are typical of west cascades forests in northwestern Oregon (Spies et al., 2018). *Arceuthobium tsugense* abundance and severity varied by stand, but was always present, even nearby our uninfected trees (see below). Fire and forest structure are the most important controls on dwarf mistletoe occurrence at the landscape scale (Shaw and Agne, 2017). *Arceuthobium tsugense* persists in fire refugia, or in areas of low burn severity, and subsequently reinvades post-disturbance likely creating the landscape distribution pattern present at the HJA (Swanson et al., 2006).

Tree Selection

We combined lidar data and aerial imagery from the HJA (Spies, 2016), to identify stands of mature and old-growth forest, across the HJA, containing *T. heterophylla*, to opportunistically select our trees, using Spies and Franklin (1991) as a

guide. We combined canopy closure values and canopy heights derived from the lidar data to find multistoried stands of non-uniform densities with the tallest trees. Dead tops and heavily infected *T. heterophylla* crowns were visible in the aerial imagery which led to final stand selections. Because *A. tsugense* abundance and severity are difficult to evaluate from remote sensing data, stands were then surveyed for dwarf mistletoe in person. To capture the full range of infection severity, trees were first rated from the ground using the Hawksworth 6-class dwarf mistletoe rating (DMR) system (Hawksworth, 1977). This involves splitting the live tree crown into thirds and assigning a score of 0, 1, or 2 to each third, and then summing these for a severity rating between 0 and 6. A score of 0 means no branches are infected, a 1 means half the branches or less are infected, and a 2 means more than half the branches are infected with dwarf mistletoe. We selected from suitable trees, picking four trees with a DMR of 0, four with DMR 1-2, four with DMR 3-4, and four with DMR 5-6 for a total of 16 trees. Tree selection criteria also included diameter (> 50 cm), height (> 35 m), and feasibility and safety of climbing. Dominant or codominant canopy position was another criteria used to select trees that are or were at point highly vigorous. Individuals with live tops and minimal bole damage or decay were prioritized to minimize confounding effects on crown structure and sapwood responses. At each tree, we inventoried a 10 – m fixed-radius plot of trees over 15 cm in diameter for estimating stand composition, stem density, and stand basal area surrounding each tree. No alternate hosts for western hemlock dwarf mistletoe, such as *Abies amabilis*, were present at these stands (Hawksworth and Wiens, 1996).

Tree Crown Measurements

Trees were rigged and then climbed using standard rope climbing techniques emphasizing climber safety; trees with root and butt rot or multiple forks were avoided. We used a simplified version of the whole-tree and crown mapping process described in Kramer et al. (2018), Van Pelt et al. (2004), and Van Pelt and Sillett (2008) and adapted it to incorporate dwarf mistletoe-related measurements. Before climbing, a functional diameter (*f*-diameter) was established to account for irregularities in ground height or stem form such as buttressing. Functional diameters were established and measured just above irregularities in stem form; if none were present, then diameter was measured at 1.37 m above the ground. Once we accessed the tree crown, the tree height was measured by dropping a fiberglass tape to the ground. This tape was affixed to the treetop and to the corresponding *f*-diameter height to provide a height reference for all branches and coring; once established, branches were measured. Branch measurements included diameter, length, slope, an estimate of foliage cover, and whether branches were live or dead (Table 1). Branch foliage cover estimates were used in place of estimates of foliage area or mass that would have required destructive sampling. Branches smaller than 4 cm in diameter were not measured but were counted. Reiterations were not encountered while measuring and are rare in *T. heterophylla* in general, so all branches are assumed typical of the species unless affected by dwarf mistletoe.

Table 1. Descriptions of measurement and their units taken on each branch.

Variable	*Units*	*Description*
Branch Diameter	centimeter	Diameter immediately distal to branch collar
Branch Length	meter	Path length of branch from bole face to tip
Slope 1	degrees	Slope of branch immediately distal to branch collar; initial angle
Slope 2	degrees	Slope of branch, from base of branch to tip of branch or center of foliage mass at tip.
Branch Foliage Cover	percent	Percent of branch length with live foliage attached to the branch
Foliage Distal to Infection	percent	Percent of live foliage occurring distal to an infection
Number of Live Branches	count	Number of live branches within the tree
Number of Dead Branches	count	Number of dead branches within the tree
Total Number of Branches	count	Total number of branches within the tree
Proportion of Live Branches	proportion of count	Number of live branches divided by the total number of branches within the tree

Branches that had developed an infection-related deformity were intensively measured to describe transformations to branch form and assess the impact of deformity volume on host function (Table 2). Deformities were defined as irregularities in typical branch structure caused by an infection such as swellings or witches' brooms (Hawksworth and Wiens, 1996). These could be identified by either living or dead aerial shoots or "basal cups" left behind where aerial shoots had emerged from the branch and subsequently detached. To calculate infection structure (deformity) volume, a length, width, and depth was measured which was then used to model an ellipsoid. These were measured in the same direction with respect to the branch, for all structures (length parallel to the branch, width perpendicular to the branch, depth perpendicular to those).

Deformities with length, width, and depth all less than 4 cm in were not measured but counted.

Table 2. Descriptions of measurements and their units taken on each dwarf mistletoe induced deformity.

Variable	*Units*	*Description*
Deformity Distance to Bole	meter	Path length along branch, from bole face to the center of a dwarf mistletoe deformity
Branch Deformity Volume	cubic meter	Volume of a dwarf mistletoe deformity modeled as an ellipsoid
Proportion of Crown in Deformity	proportion	Total volume of deformities in the tree divided by the total volume of the crown
Dwarf Mistletoe Infections	count	Sum of all dwarf mistletoe deformity volumes within the tree

Surveys of other tree species infected with dwarf mistletoes have found consistently replicated, distinct deformations to branch structure thought to be a characteristic of that host-pathosystem (Geils et al., 2002). While classes have been previously described for non-systemic dwarf mistletoes, they did not adequately capture the deformations we observed in *T. heterophylla* crowns (Geils et al., 2002; Hawksworth, 1961). Deformities were classified using a system we developed, that represented four distinct classes: “classic broom”, “platform”, “pendulous”, or “spindle” (Figure 5). The same climber classified deformities in all trees to reduce sampling bias and variation. In some instances, deformities were clustered or otherwise difficult to distinguish as arising from an individual infection, so judgement of the climber was used to delineate structures, and to classify and measure them.

Figure 5. The four deformity classes found within our *T. heterophylla* infected crowns: platform (top left), classic broom (top right), pendulous (lower left), and spindle (lower right). Note the foliage and branchlets of the classic extend away from the bole leaving one side bare while the pendulous has a skirt of foliage all around it. The classic and spindle are both exhibiting secondary infection.

Crown Volume

We utilized derived crown width measurements from crown mapping to capture stochastic differences in tree crown form by modeling 5-meter paraboloid frusta for the length of the live crown. The base of the live crown was defined as the lowest living branch (Shinozaki et al., 1964b). Crown widths were calculated from individual branch slope measurements and then averaged in 5-meter intervals. These widths were used to

model the parabolic frusta and summed for the whole tree. This frusta-summation method estimated smaller crown volumes than the commonly used parabolic method (Van Pelt and North, 1999) and we assume was better suited to the stochastic crowns. The crown volume metrics measured included minimum branch height, crown depth, crown volume, and sapwood area at DBH and live crown base (Table 3).

Core Sampling

We collected two tree cores at the *f*-diameter and two cores at the base of the live crown from each tree to examine a mechanism for trees to compensate for infection-induced reductions to whole tree water use by measuring sapwood area (Meinzer et al., 2004). Sapwood area may also reflect other alterations to hydraulic architecture such as reductions in foliage (Shinozaki et al., 1964a). We also measured the 10-year basal area increment (BAI) and calculated the relative basal area increment (RBAI) to examine growth trends related to infection severity. All coring was completed during September 2019 to minimize variation from different seasonal availability of water and bole growth. Diameter of the bole at the coring location was taken at the narrowest point when branches or stem irregularities were present. The sapwood length was measured in the field to avoid drying-related shrinkage. Sapwood was determined by holding the fresh core up to a light source and examining the core for the sapwood – heartwood boundary. These cores were saved for later BAI measurements and cross-dating to determine ages. Occasionally wetwood was encountered in tree cores. Wetwood is a phenomenon in western hemlocks where sapwood is converted to heartwood and then moisture, phenols

and other compounds concentrate there. This results in an abnormally moist portion of heartwood and is often associated with ring shake and defense against rot-associated fungus (Shaw et al., 1995).

Table 3. Descriptions of measurements taken on the tree crown and sapwood.

Variable	*Units*	*Description*
Minimum Branch Height	meter	Lowest live branch on the tree; base of live crown
Crown Depth	meter	Tree height minus the height of live crown base
Crown Volume	cubic meter	Sum of crown volume frusta, modeled as paraboloids in 5-meter segments or as a whole paraboloid
Sapwood Area at *f* DBH	square meter	Sapwood area measured from cores taken at the functional breast height.
Relative Sapwood Area at *f* DBH	unitless	Sapwood area divided by the total basal area of the tree stem at the functional breast height.
Sapwood Area at Live Crown Base	square meter	Sapwood area measured from cores taken at the base of the live crown.
Relative Sapwood Area at Live Crown Base	unitless	Sapwood area divided by the total basal area of the tree stem at the base of the live crown.

Analysis

A series of linear (LM) and generalized linear models (GLM) were fit to estimate mean responses among the 16 western hemlocks where branch severity, foliage severity, or incidence were explanatory variables (Table 4). These three measures reflect the process of infection intensification, where ejected seeds land on branches of the original host and infect new branches or reinfect the source branch, increasing incidence and/or severity *within* a tree crown (Geils et al., 2002). Branch severity was used to represent a fine-scale version of the DMR system which is the current standard for measuring infection severity (Hawksworth, 1977). Because foliage distal to infection was reported

have reduced physiological function, foliage severity was used to represent where infection impacts would be most strongly associated (Meinzer et al., 2004). Incidence is another way of measuring the intensification process which we compare to the other two measures of severity.

Table 4. Descriptions of the explanatory variables and their units used in the modeling.

Variable	*Units*	*Description*
Branch Severity	percentage	Number of live, infected branches divided by number of live branches
Foliage Severity	percentage	Number of live, infected branches with effected foliage greater than 33%, divided by the number of live branches
Incidence	count	Total number of infections on live branches within a tree

It was not possible to include all explanatory variables in one model and capture their interactions due to limited sample size and power, so all responses were tested with each measure of severity. The general form of the linear and generalized linear model for estimating effects of infection intensification:

$$= \beta_1(Branch, Foliage\ Severity\ or\ Incidence) + \beta_0$$

Estimated values for the coefficient β_1 are presented below. We fit a quasibinomial GLM for proportion of live branches as the response with a logit link and fit negative binomial GLMs for the number of live branches, number of dead branches, total number of branches, and median number of infections per branch with a natural logarithm link (Ramsey and Schafer, 2012). Slope estimates from the binomial model with a logit link are estimated odd ratios. Slope estimates from negative binomial models with a natural logarithm link are multiplicative changes in mean response. All other

responses were modeled by fitting an LM: average, median, and max branch diameter; average, median, and max branch length; average and median branch slope 1; average and median branch slope 2; average branch foliage; average deformity distance to bole; average branch deformity volume; total deformity volume; minimum branch height; crown depth; total crown volume; proportion of crown volume in deformity; sapwood area at *f*-DBH and live crown base; relative sapwood area at *f*-DBH and live crown base.

We then compared each model's fit using the amount of variation explained by the explanatory variables (R^2). To compare different model types, we used the theoretical R^2 for the negative binomial and quasibinomial GLMs (Nakagawa et al., 2017; Nakagawa and Schielzeth, 2013). To determine if *A. tsugense* was exhibiting an influence on a specific response, we used a minimum R^2 of 0.20. Forest development processes often lead to surviving trees with individualistic and irregular tree crowns, of which dwarf mistletoe infection is one process (Michel and Winter, 2009; Van Pelt and Sillett, 2008). Additionally, there are no previous studies to suggest what amount of association should be expected with a continuous measure of severity, so we propose an R^2 of 0.2 is an appropriate starting place.

Residuals for the LMs were examined graphically for assumptions of constant variance and normality. Residual vs deviance residual plots were examined for each GLM and no unusual patterns were observed. Overdispersion was checked for each GLM with a negative binomial and binomial distribution. Only the GLM with counted proportion of live branches as the response variable was found to have a high measure of overdispersion (> 5.0) and so a quasibinomial correction was used for final analyses and

reporting (Ramsey and Schafer, 2012). All analyses were performed using R version 3.6.3 (R Core Team, 2019). Negative binomial GLMs were fit with the MASS package version 7.3-47 (Venables and Ripley, 2002). Theoretical R^2 was calculated for the negative binomial and quasibinomial GLMs using the MuMIn package (Barton, 2019).

Results

Trees in our dataset captured a range of age, height, diameter expected in old and mature forests, and the full range of infection severity (Table 5). No evidence of decay was present in the roots of trees and extensive coring revealed no evidence of decay at the base of the live crown and at the *f*-diameter. Tree 12 exhibited a dead top, a common symptom associated with extensive *A. tsugense* infection (Hawksworth and Wiens, 1996). Frequently, models where branch or foliage severity were explanatory variables, produced R^2 values larger than those same models with incidence. However, the likelihood of the number of dead branches, was most strongly associated with incidence.

Table 5. Characteristics of the 16 *T. heterophylla* sample trees arranged by age, with tree height, functional diameter, density of all trees around each hemlock, basal area of the stand surrounding each hemlock, crown volume, branch severity (the proportion of all live branches infected), foliage severity (the proportion of all live branches with 33% or more foliage affected by infection), and incidence (total number of individual infections on live branches).

Tree	*Age*	*Tree Height m*	*f-Diameter cm*	*Density* $t \cdot ha^{-1}$	*Basal Area* $m^2 \cdot ha^{-1}$	*Crown Volume* m^3	*Branch Severity %*	*Foliage Severity %*	*Incidence*
1	97	48.8	96.0	159	8.70	1955.0	0	0	0
2	116	46.6	76.5	191	9.30	1658.8	0	0	0
3	125	35.5	63.1	223	23.40	1864.8	0	0	0
4	144	43.8	71.8	318	9.20	1813.0	58	23	427
5	145	40.4	58.5	350	34.00	980.7	100	100	875
6	160	51.6	85.8	95	4.90	1551.4	100	100	1489
7	163	42.7	82.2	159	24.50	2123.2	100	98	3615
8	164	40.5	67.5	350	37.20	1803.6	89	57	786
9	174	38.6	60.5	255	52.50	2086.7	75	38	764
10	176	46.8	83.8	446	36.70	1923.0	73	58	1479
11	179	44.4	81.2	64	4.50	1335.2	16	1	23
12	207	49.2	96.3	127	12.80	520.7	100	97	813
13	221	48.7	82.5	637	103.20	947.2	64	52	662
14	222	54.7	104.5	159	80.30	1651.4	25	0	69
15	250	33.0	70.1	255	12.50	698.7	100	100	1405
16	321	52.0	83.1	191	14.90	2718.7	0	0	0

Branch Modeling

Changes in mean average branch foliage, followed by branch slopes 1 and 2 were best estimated by dwarf mistletoe branch and foliage severity models (Table 6). The number of live and dead branches reported the next strongest R^2 values, although they were below the 0.2 threshold (Appendix A). The proportion of live branches, total number of branches had weak associations ($R^2 < 0.2$), and branch diameter and length were reported very weak relationships ($R^2 < 0.1$). We estimated a reduction in mean average branch foliage of -13.39 percent (95% CI -19.27, -7.51) for the foliage severity model as infection severity increased from 0 to 100 percent ($R^2 = 0.63$, Figure 6).

Table 6. Results from modeling for the set of branch-related response variables. The fixed effect with the highest degree of evidence (measured by R^2) of the three is listed with the estimated slope, 95% confidence intervals, test statistics and R^2. Coefficient estimates represent a shift in response variables for a change in severity of 0 to 100%. Full set of model results in Appendix A.

Response	Model Type	Fixed Effect	Coefficient Estimate	Low 95% CI	High 95% CI	F	df	p	R^2
Average Branch Foliage	LM	Foliage Severity	-13.39	-19.27	-7.51	23.82	1, 14	0.000	0.63
Average Slope 1	LM	Branch Severity	7.02	-0.56	14.61	3.95	1, 14	0.067	0.22
Median Slope 1	LM	Branch Severity	7.04	-0.40	14.48	4.11	1, 14	0.062	0.23
Median Slope 2	LM	Foliage Severity	-13.51	-28.81	1.80	3.58	1, 14	0.079	0.20

Results from branch slope modeling showed crown profiles may be compacting, losing typical conical shape as they became more heavily infected with *A. tsugense*. Branch severity models of mean average and median slope 1 estimated an increase in

slope angle of 7.02 (95% CI -0.56, 14.61) and 7.04 (95% CI -0.40, 14.48) as severity increased from 0 to 100 percent, respectively (R^2 = 0.22 and 0.23). Foliage severity similarly estimated an increase but with a weaker relationship. Meanwhile, foliage severity models of median slope 2 estimated a decrease in slope angle of -13.51 (95% CI -28.81, 1.80) as severity increased from 0 to 100 percent (R^2 = 0.20). Branch severity also estimated a decrease, but with a weaker relationship; incidence reported a weak relationship for all three of these estimates.

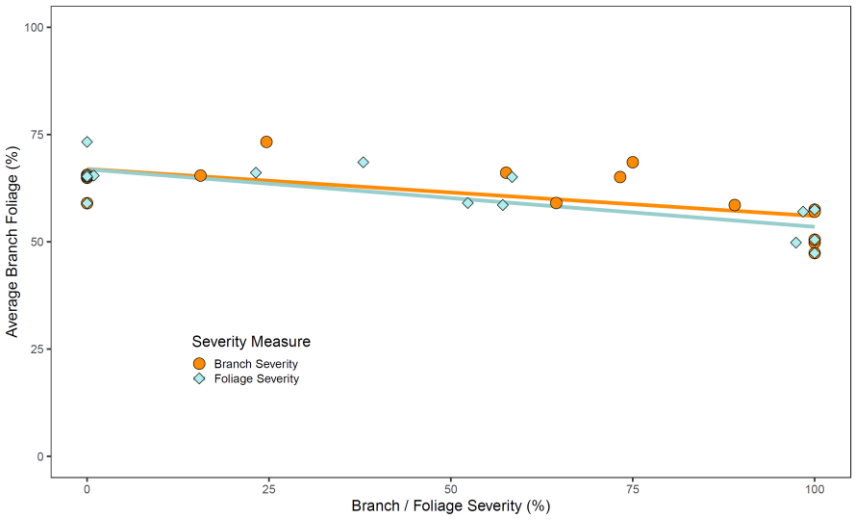

Figure 6. Models of mean average branch foliage cover with branch severity (orange lines, % live branches with infection) and foliage severity (blue lines, % live branches with 33% or more foliage affected by infection) as explanatory variables. Raw data is plotted alongside models with branch severity (orange circles) or foliage severity (blue diamonds).

Results from both our branch and foliage severity models estimated similar changes to the number of live and dead branches (Figure 7, Appendix A). A 0.76-fold (95% CI 0.55, 1.06) reduction in the mean number of live branches was estimated by the branch and foliage severity models, as severity increased from 0 to 100 percent. Our

branch severity model estimated a 1.36-fold (95% CI 0.89, 2.08) increase and our foliage severity model estimated a 1.37-fold (95% CI 0.92, 2.04) increase in the mean number of dead branches, as severity increased from 0 to 100 percent. However, these estimates showed weak evidence of correlation. R^2 values for the branch severity models were 0.14 for the number of live and 0.11 for the number of dead branches; for the foliage severity models were 0.14 for the number of live and 0.13 for the number of dead branches; the incidence model for mean number of live branches did not meet assumptions and an R^2 of 0.14 for number of dead branches was highest among the three explanatory variables. No evidence was found for the estimated decrease in the proportion of live branches ($R^2 \leq 0.01$).

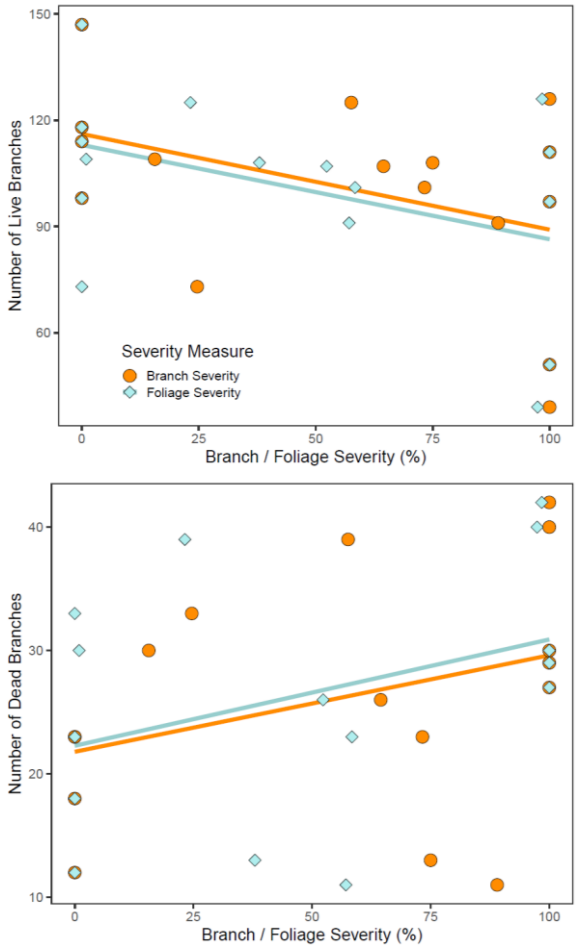

Figure 7. Models of mean number of live (top) and dead branches (bottom) with dwarf mistletoe branch severity (orange lines, % live branches with infection) and foliage severity (blue lines, % live branches with 33% or more foliage affected by infection) as explanatory variables. Raw data is plotted alongside models with branch severity (orange circles) or foliage severity (blue diamonds).

Deformity Modeling

Deformity-related response variables produced models with our highest degrees of evidence (Table 7, Appendix B). As expected, an increase in branch severity, foliage severity, and incidence resulted in an increase in the median number of dwarf mistletoe infections per branch (Figure 8). The branch severity model estimated branches to

experience a 27-fold (95% CI 9.60, 90.06) increase in the median number of infections, as severity increased from 0 to 100 percent (R^2 = 0.78). The model with incidence reported the highest degree of evidence of all incidence models with an of R^2 0.49.

Table 7. Results from modeling for the set of deformity – related response variables. The fixed effect with the highest degree of evidence (measured by R^2) of the three is listed with the estimated slope, 95% confidence intervals, test statistics and R^2. Coefficient estimates represent a shift in response variables for a change in severity of 0 to 100%. Full set of model results in Appendix B.

Response	Model Type	Fixed Effect	Coefficient Estimate	Low 95% CI	High 95% CI	F	df	$\chi 2$	p	R^2
Median Dwarf Mistletoe Infection	GLM	Branch Severity	27.20	9.60	90.06	---	1	23.98	0.000	0.78
Total Deformity Volume	LM	Foliage Severity	55.12	33.54	76.70	30.00	1, 14	---	0.000	0.68
Proportion of Crown in Deformity	LM	Foliage Severity	0.07	0.04	0.11	18.85	1, 14	---	0.001	0.57
Average Deformity Distance to Bole	LM	Branch Severity	3.17	1.62	4.70	19.43	1, 14	---	0.001	0.58

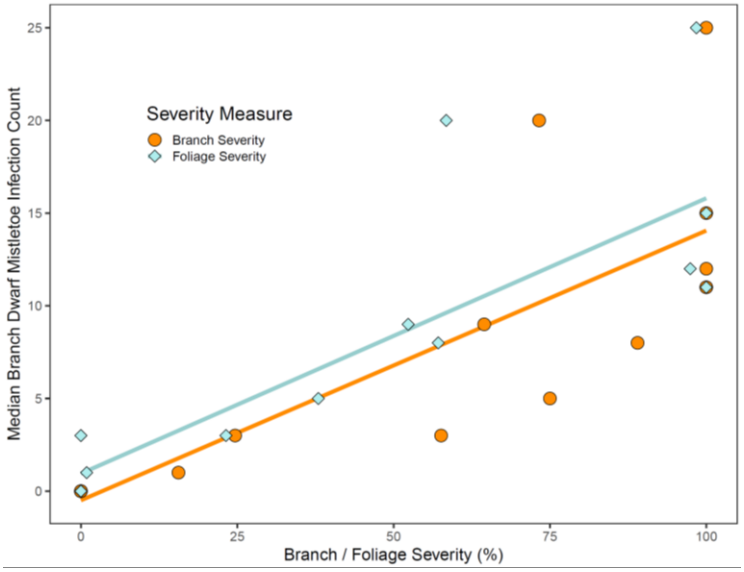

Figure 8. Models of median branch dwarf mistletoe infection count with dwarf mistletoe branch severity (orange lines, % live branches with infection) and foliage severity (blue lines, % live branches with 33% or more foliage affected by infection) as explanatory variables. Raw data is plotted alongside models with branch severity (orange circles) or foliage severity (blue diamonds).

A small amount of a dwarf mistletoe infected *T. heterophylla* crown volume is comprised of deformities (Figure 9). Total deformity volumes only ranged from 0.56 m^3 to 75.59 m^3 while total crown volumes ranged from 520.70 m^3 to 2132.20 m^3 in dwarf mistletoe infected trees. We estimated an increase in mean total deformity volume of 55.12 m^3 (95% CI 33.54, 76.70) as foliage severity increased from 0 to 100 percent (R^2 = 0.68). As the total deformity volume in a *T. heterophylla* crown increased, so too did the proportion of the crown comprised of deformities. Foliage severity models estimated an increase of 7 percent (95% CI 4, 11) in proportion of crown comprised of deformities (R^2 = 0.57). However, incidence, branch severity, and foliage severity were estimated to have essentially no effect on the mean average branch deformity volume and exhibited weak evidence for a relationship in those models (Appendix B). Examining the allocation of

deformity volume by height showed variation in the location of deformity volume in the crowns of infected trees but appears localized to the mid-crown of the infected trees (Figure 10). The branch severity model estimated an increase in mean average deformity distance to bole of 3.17 m (95% CI 1.62, 4.70), as infection severity increased from 0 to 100 percent (R^2 = 0.58).

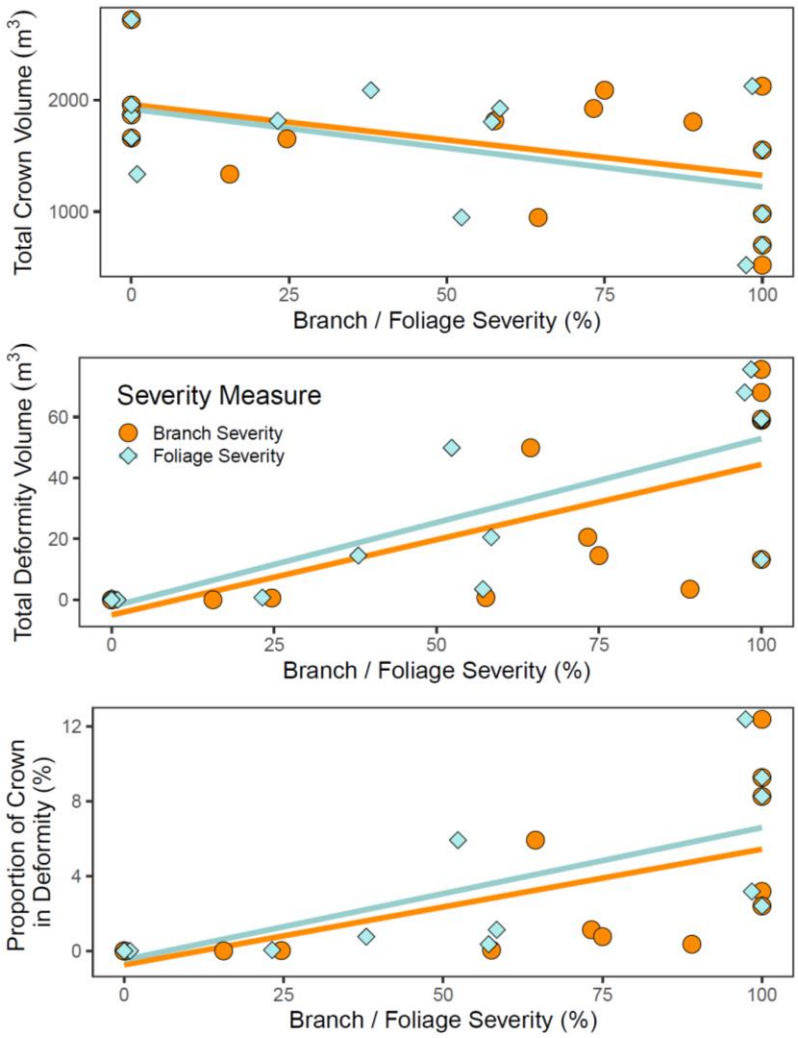

Figure 9. Models of mean total crown volume (top), total deformity volume (middle), and proportion of crown composed of deformities (bottom) with branch severity (orange lines, % live branches with infection) and foliage severity (blue lines, % live branches with 33% or more foliage affected by infection) as explanatory variables. Raw data is

plotted alongside models with branch severity (orange circles) or foliage severity (blue diamonds). As infection severity increases, volume of the tree's crown decreases and total deformity volume increases resulting in an increased proportion of crown volume filled by deformities.

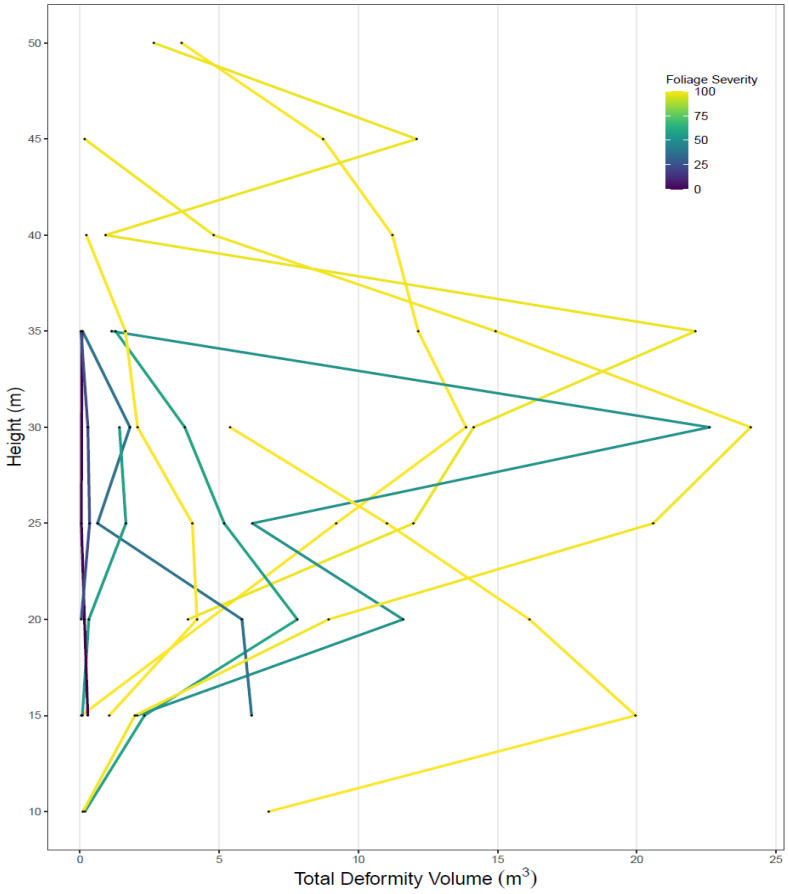

Figure 10. Deformity volumes summed at 5-meter intervals and plotted against their height. Each 5-meter mark on the vertical axis represents the 5 meters below it. Each line represents one of the 12 infected trees in this study, colored by their foliage severity (% live branches with 33% or more foliage affected by infection) where yellow colors are highest severity and blues and purples are lowest severity. Each data point represents a deformity volume summation. Trees varied widely where the deformity volume was located within the crown, but most of the volume was concentrated in the middle third of the crown.

Deformity Class

Deformity class did not exhibit evidence for a relationship to average deformity distance to bole (Table 8). Except for the spindle class, deformity class had negligible effects on mean average deformity volume. Of the deformities large enough to measure volume (≥ 4 cm in one dimension), we counted 932 classic brooms, 724 platforms, 400 pendulous-shaped, 7 spindle-shaped, and 1 bole infection across all trees. The spindle class represented the smallest amount of total volume of all the classes and were smallest on average, but they were much more abundant than it appears because they were small and we only tallied incidence for small infections. A pendulum infection created the largest max volume of any deformity. The four classes were also found at least 2.51 m from the bole on average.

Table 8. Summary table of statistics for each deformity class within infected tree crowns with number observed, average and maximum deformity volume modeled as an ellipsoid, average distance to bole, average height, and their standard deviations listed in parentheses.

Deformity Class	n	Average Volume m^3	Max Volume m3	Average Distance to Bole m	Average Height m
Classic	932	0.19 (± 0.28)	2.95	3.49 (± 1.56)	26.07 (± 9.00)
Platform	724	0.14 (± 0.19)	2.83	3.00 (± 1.52)	28.39 (± 9.28)
Pendulous	400	0.20 (± 0.37)	5.74	3.56 (± 1.68)	25.93 (± 8.29)
Spindle	7	0.003 (± 0.001)	0.003	2.51 (± 1.54)	17.78 (± 5.37)

Crown, Whole tree, and Sapwood Modeling

Every model with incidence as an explanatory variable showed almost no evidence for a relationship to total crown volume, crown depth, minimum branch height, and relative or absolute sapwood area (Appendix C). Models estimating changes in mean

total crown volume with dwarf mistletoe branch and foliage severity as explanatory variables, exhibited our strongest evidence for a relationship in this set of responses (Table 9, Appendix C). Both estimated similar reductions in mean total crown volume of -632.87 m^3 (95% CI -1330.30, 64.57) for branch severity and -696.34 m^3 (95% CI -1357.10, -35.58) for foliage severity as infection severity increased from 0 – 100 percent (Figure 9, top). Total crown volume and volume allocation by height showed a wide variation, regardless of dwarf mistletoe infection severity. Similar to deformity volume, crown volume appeared to be concentrated in the lower and middle thirds of the crown, across the infection severity gradient (Figure 11).

Table 9. Results from modeling for the set of whole tree and sapwood area response variables. The fixed effect with the highest degree of evidence (measured by R^2) of the three is listed with the estimated slope, 95% confidence intervals, test statistics and R^2. Coefficient estimates represent a shift in response variables for a change in severity of 0 to 100%. Full set of model results in Appendix C

Response	Model Type	Fixed Effect	Coefficient Estimate	Low 95% CI	High 95% CI	F	df	p	R^2
Frusta-based Crown Volume	LM	Foliage Severity	-696.34	-1357.10	-35.58	7.72	1, 14	0.040	0.27
Crown Depth	LM	Branch Severity	-6.25	-13.19	0.70	3.72	1, 14	0.074	0.21

In addition to estimated reductions in mean total crown volume, crown depth is also estimated to decrease as dwarf mistletoe branch and foliage severity increases (Table 9). We estimated a reduction in mean crown depth of -6.25 m (95% CI -13.19, 0.70) as infection severity increased from 0 – 100 percent (R^2 = 0.21). Mean minimum branch height was estimated to increase but showed weak evidence for a relationship to infection severity in our models ($R^2 \leq 0.07$). Both of these results suggest branches may be thinned from below as infection severity increases.

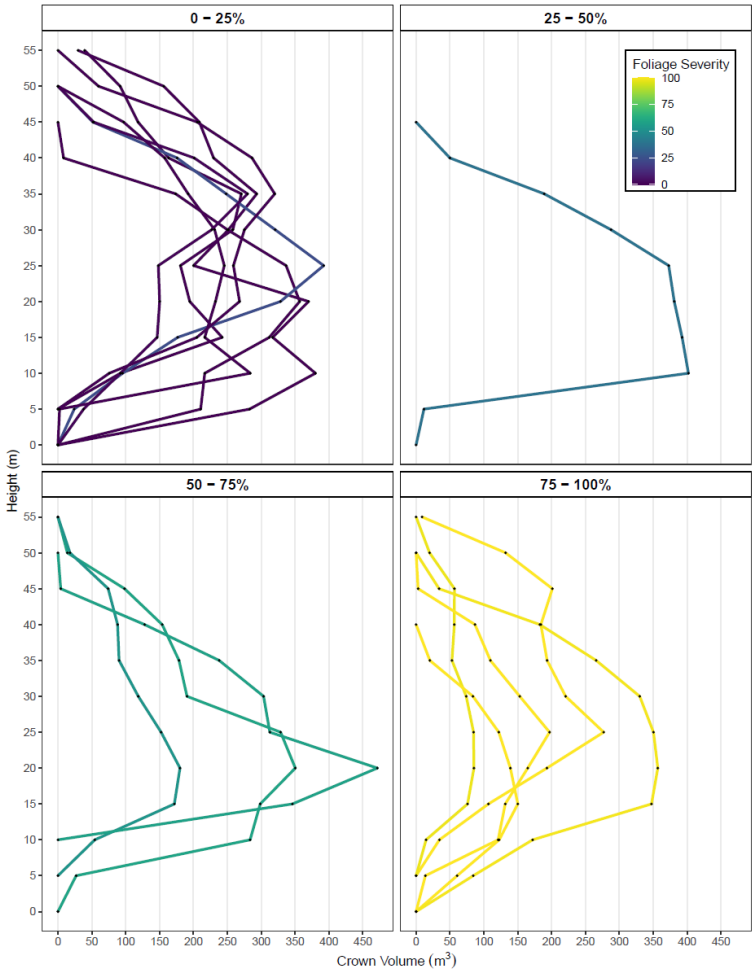

Figure 11. Crown volume, modeled as frusta of a paraboloid in 5-meter bins, using crown width data, plotted against height of that frusta in the tree. Each 5-meter mark on the vertical axis represents the 5 meters below it. Each line represents one of the 16 trees in this study and trees have been grouped into 4 groups for ease of viewing, corresponding to their foliage severity (% live branches with 33% or more foliage affected by infection): yellow colors are highest severity and blues and purples are lowest severity. Each data point represents an individual frustum.

Models of relative sapwood area at *f*-diameter and at live crown base had almost no evidence for a relationship ($R^2 \leq 0.01$) while estimating practically insignificant reductions in area (Appendix C). Models of mean absolute sapwood area produced higher, but still weak degrees of evidence ($R^2 \leq 0.11$). The models of mean absolute

sapwood area also estimated a practically insignificant change in area associated with increases in all three explanatory variables. We performed an additional exploratory analysis to examine if the pipe-model theory was evidenced in our sample trees, utilizing the number of live branches as an explanatory variable in place of the area or mass of live foliage. Modeling relative sapwood area at the *f*-diameter and at the base of live crown, with the number of live branches of each tree as the explanatory variable, exhibited stronger evidence for a relationship than branch severity, foliage severity, or incidence (R^2 at f-diameter = 0.23, R^2 at base of live crown = 0.33). These models estimated increases in relative sapwood area as the number of live branches increased, without accounting for dwarf mistletoe infection severity or incidence (Figure 12). Tree RBAI was estimated to decrease with increasing infection severity. Only the model with foliage severity as an explanatory variable met our threshold, with an R^2 of 0.20. This low degree of evidence was likely due to the wide variation in RBAI for uninfected trees, ranging from 0.002 to 0.02, or very low to very high amount of radial growth. However, all the trees with foliage severity greater than 90% had an RBAI of less than 0.08.

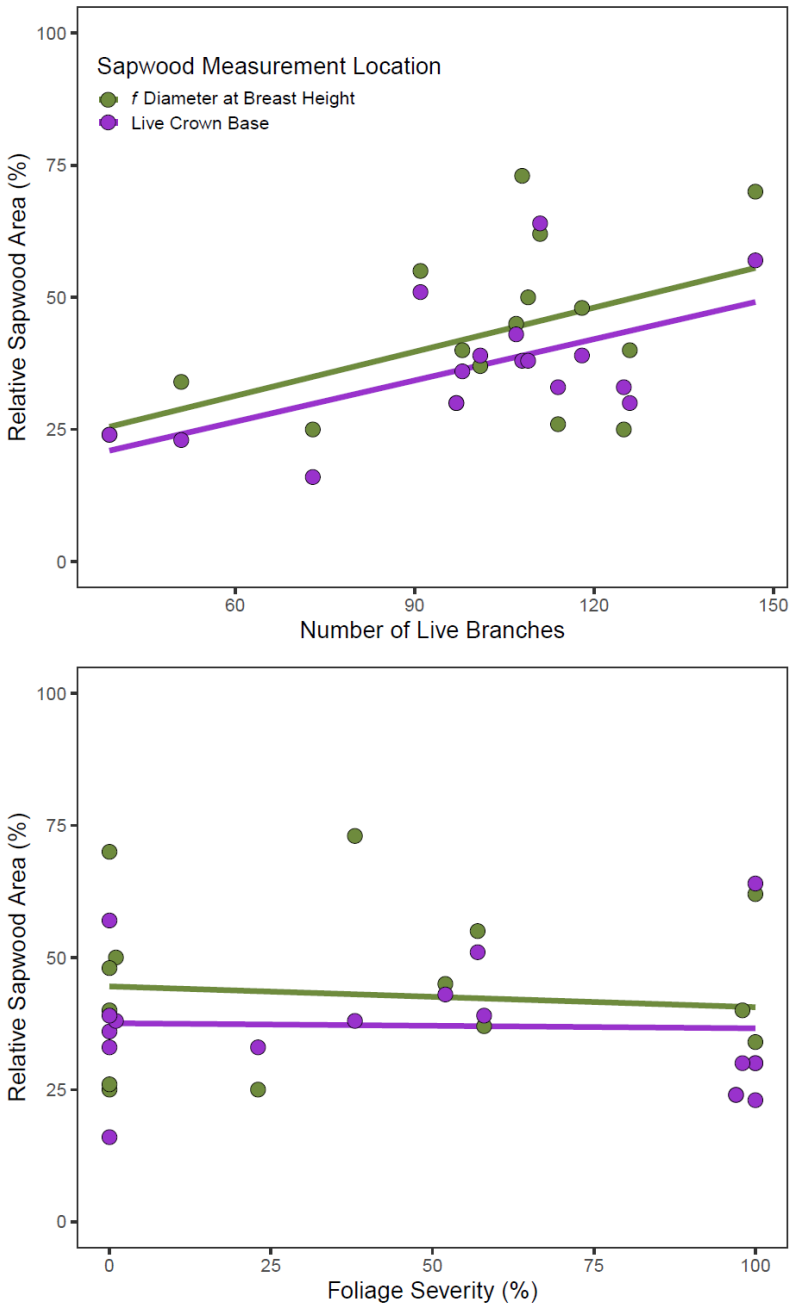

Figure 12. Relative sapwood area models with the number of live branches as the explanatory variable (top) and foliage severity (% live branches with 33% or more foliage affected by infection, bottom). Models for the relative sapwood at the functional diameter (green lines and circles) and live crown base (purple lines and circles) are displayed with the raw data.

Discussion

From the branch to whole tree level, *A. tsugense* exerts a profound influence on *T. heterophylla* trees as infection intensifies in the tree crown. Our results suggest shifts in crown structure imply a shift in function, from biomass production and growth, to survival. Infected trees experienced a decrease in average branch foliage cover with increasing infection severity (Figure 6), and in the most severely infected trees, almost all live foliage was located distal to an *A. tsugense* infection (Figure 13). Whole tree foliage has been suggested to be reduced by an increase in branch mortality due to high infection severity, but we found weak evidence for decreased live branches. Direct impacts to crown form were not clear, but crowns experienced an apparent compaction due to increasingly downward branch slopes and a rising base of live crown resulting in reduced crown volumes. Increasing severity led to increasing deformity volume and crowns that were increasingly comprised of deformities. Sapwood area was unrelated to infection severity suggesting in foliage cover may allow the trees to compensate for the water and nutrient loss.

This study was exploratory in nature and is the first to apply the canopy mapping process to examine the transformation of mature and old growth *T. heterophylla* crown architecture through a fine-scale gradient of infection severity by *A. tsugense*. As such, there is a lack of comparable literature for this present study although *A. tsugense* is well studied (Muir and Hennon, 2007).

Foliage Impacts

Dwarf mistletoe infections continually influence water and nutrient dynamics in their host, resulting in shifts of hydraulic architecture that allow the tree to maintain some form of water homeostasis (Hawksworth and Wiens, 1996; Meinzer et al., 2004; Sala et al., 2001). Meinzer et al. (2004) observed that old *T. heterophylla* infected by *A. tsugense* experienced reductions in branch foliage that preserved leaf-specific conductivity in infected branches and whole tree foliage due to a loss of live branches in infected trees. The remaining branch foliage distal to infection was found to contain almost half the nitrogen, likely influenced by the mistletoe. This decrease in foliage and photosynthetic capacity is thought to render infected trees unable to meet the respiratory demands of live branches and support *A. tsugense* infections during stress events, resulting in branch dieback and reductions in tree growth (Bell et al., 2020; Marias et al., 2014; Meinzer et al., 2004). Our results show compelling evidence that *T. heterophylla* experience reductions in branch foliage cover due to of infection intensification, although the average reduction was only ~ 13% (Figure 6). Additionally, almost all remaining foliage in 100% branch severity trees was found distal to infections (Figure 13), suggesting these trees are experiencing severely reduced photosynthetic capacity.

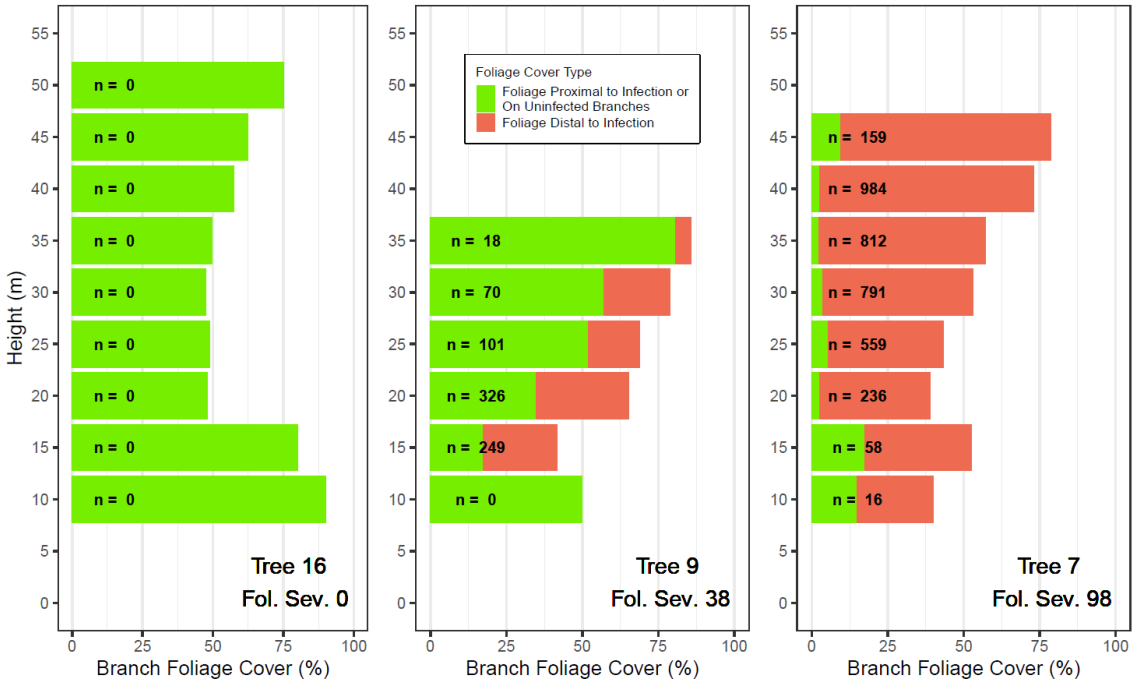

Figure 13. Branch foliage cover proximal and distal to infection, or on uninfected branches, stacked, with both summing to total branch foliage cover, averaged in 5 – meter intervals for the three trees with the largest crown volumes. The n represents the number of live infections in that 5 – meter interval. Trees increase in infection severity from left to right. Trees are labeled with their corresponding tree number and their foliage severity from Table 5.

While our models also estimated a decrease in live branches and an increase in dead branches, likely resulting in reduced whole tree foliage, we found weak evidence of correlation with infection severity and estimated a wide range of plausible values for the slopes of both models (Figure 7). This suggests, despite the average reduction in branch foliage cover and reduced photosynthetic capacity of remaining needles, infected trees in this study are still capable of meeting the respiratory demands of all branches and that branch mortality may not be a direct result of infection intensification. Branches of *T. heterophylla* have been reported to be kept alive and foliated, below zones of

prohibitively low light where other uninfected branches would have been shaded out (Muir and Hennon, 2007). Further, reductions to whole tree foliage may manifest from reductions in individual branch foliage cover across the whole tree. Tree selection bias likely limits the scope of this finding though, as safer trees to climb usually have fewer dead branches and may be more vigorous. Studies, such as Meinzer et al. (2004), that can access severely infected trees without this bias and without felling, may have a more accurate representation of branch mortality.

Foliage impacts are not consistent throughout the other dwarf mistletoe – host pathosystems, though available literature on foliage impacts is limited. Sala et al. (2001) found the opposite effect of our results on foliage when measuring changes to the leaf area: sapwood area ratio of *Pseudotsuga menziesii* infected with *A. douglasii* which creates a systemic infection, and *Larix occidentalis* infected with *A. laricis*, which creates non-systemic infections, in mixed conifer forests. In both tree species, high infection severity was associated with increases in the leaf area: sapwood area ratio due to increases in leaf area. Godfree et al. (2003), examined how the abundance of *A. americanum* affected the canopy structure of an old growth *Pinus contorta* var. *murrayana* forest in central Oregon. They found severe infections were associated with a stand-wide, skew of foliage distribution to lower heights in the canopy but made no determinations about changes in total foliage mass or area. Most recently Hoffman et al. (2007), in a study on *A. vaginatum*'s influence on fire in *P. ponderosa* forest stands, found canopy foliage mass remained unchanged despite infection severity. This suggests impacts of a dwarf mistletoe on its host may be specific to the host and pathogen.

Research that tracks branch foliage and mortality over time through infection intensification and can link those to physiological impacts, would provide significant clarity to the impact of *A. tsugense* on host growth. Our study only captures a point in time, the time of initial infection is unknown, complicating this picture. The epidemiology of dwarf mistletoe involves spread into new hosts and intensification within the existing host (Hawksworth and Wiens, 1996; Shaw and Mathiasen, 2013). Impacts of infections on host trees change through time as tree infection intensifies. During initial stages of infection, there may be increased growth associated with low severity, but at high severity there is typically severely decreased growth (Marias et al., 2014).

The location of initial infection may also alter the impacts. For example, initial infections lower in the tree crown may be outgrown by *T. heterophylla* as height growth of uninfected tops outpaces the rate of upward spread of infection (Muir and Hennon, 2007). Once height growth slows, total infection of the crown is possible (Robinson and Geils, 2006). Meinzer et al. (2004) also suggests transient changes to the leaf area: sapwood area ratio may produce apparent discrepancies in tree allometric responses to infection which we could not observe without repeated measurements.

Crown Structure and Volume

Counter to expectations, we did not observe evidence for an effect of increasing infection severity on the mean average, max, or median branch diameter or length. The only study that examined *A. tsugense*'s effects on *T. heterophylla* branches, measured 30

trees averaging 110 years old from dominant and codominant positions and reported increases in branch diameter, immediately distal to the branch collar, as severity increased (Smith, 1969). Estimates of branch slope angle to tip (slope 2) suggest branch tips end up closer to the tree bole and ground due to increasing infection severity than would be expected for the typical branch arrangement in uninfected trees that maximizes light interception (Smith and Brewer, 1994). Some deformities have been observed to weigh up to several hundred kilograms and this additional weight on the tips of branches may result in a branch droop (Muir and Hennon, 2007). The estimated increased initial branch slope angle (slope 1) with increasing infection severity may be a compensating mechanism for the branch to handle the added weight. Wellwood (1956) observed more compression wood within trees' stems, on the side nearest to infected branches, further suggesting decreased slope 2 angles may be a weight related phenomenon.

Estimates of decreases in crown depth also run counter to previous findings of changes to crown structure. Previous reviews of *A. tsugense*'s whole tree effects on *T. heterophylla* have described increasing infection severity may lower the base of the live crown due to branches kept alive below the height where uninfected branches would self-thin (Geils et al., 2002; Muir and Hennon, 2007; Shaw and Agne, 2017). Our results suggest the base of the live crown may actually be increasing in height, although estimates for increases in minimum branch height were not well supported. Decreasing crown depth may also shift canopy volume allocation higher in the trees, despite decreasing branch slope 2 angles, but this was not clear from our findings (Figure 11). The lack of compelling evidence for an effect on branch mortality, which would drive

shifts in crown depth, suggest differences in crown depth are more likely attributable to environmental factors than infection severity.

Infection severity exhibited a negative influence on crown volume, although, of the completely infected trees (branch severity = 100%), a wide range of total volumes was observed. The smallest crown volume we observed overall was of a completely infected tree at 520.7 m^3. The largest completely infected crown had a volume of 2123.2 m^3, second largest overall and the same tree with the highest incidence (Table 5). In all our trees, crown volume allocation by height varied across all infection severities reflecting the stochastic nature of crown development processes in mature and old growth forests (Reilly and Spies, 2015), but crown volume appeared to be greatest in the low to mid crown (Figure 11). Clearly environmental factors, tree vigor, and time since infection are exhibiting influences on the crown volume and structure, but we found evidence to support an overall negative effect of dwarf mistletoe on crown volume. Agne et al. (2014) found strong evidence that in stands of *Pinus contorta* subsp. *murrayana* infected with *A. americanum*, canopy volume and cohort height decreased as infection severity increased. Godfree et al. (2003, 2002) found evidence that individual tree crown volume may be reduced by high severity dwarf mistletoe infections, but that total canopy volume remained constant in their stand due to demographic shifts in tree size classes.

Branch slope, crown depth, and crown volume model results, as well as increased difficulty maneuvering within the heavily infected crowns, suggest an overall compaction of *T. heterophylla* crowns due to increasing *A. tsugense* infection severity. The compaction of infected *T. heterophylla* crowns could have implications for biota that

utilize deformities for habitat or forage (Hawksworth and Wiens, 1996; Muir and Hennon, 2007), for spread and intensification of *A. tsugense* (Parmeter, 1978; Robinson and Geils, 2006), and for fire and fuels in forests (Shaw and Agne, 2017). *Arceuthobium tsugense*'s role in development of old growth structure in Pacific Northwest forests has largely been attributed to gap creation caused by host mortality (Mathiasen et al., 2008; Reilly and Spies, 2016), but compacting crowns as infection severity increases suggest a continuous process of increasing space between tree crowns before mortality occurs. This would allow more light to reach the forest floor in between trees, especially under the canopies of *T. heterophylla* dominated forests where light penetration is low (Reilly and Spies, 2015).

While crowns were decreased in size and spread, total deformity volume was estimated to increase as infection severity increased, resulting in an increased proportion of crown volume taken up by deformities (Figure 9). Increasing infection severity and total deformity volume did not coincide with an increase in average branch deformity volume, suggesting that infection intensification within the tree crown is the main contributor to total deformity volume and not all infections form large deformities. The lack of effect of infection severity on average deformity volume suggests the development of deformities may be driven instead by light, temperature, or productivity of foliage, all factors important for *A. tsugense*'s development and related to an infection's height within the canopy (Shaw and Weiss, 2000). Trees with the greatest infection severity had a 27-fold increase in the median number of infections per branch when compared to uninfected trees and we expected that increasing infection incidence

would result in increasing branch deformity volume (Figure 8). The distribution of deformity volume within *T. heterophylla* crowns varied by height, independent of infection severity but appeared localized to the low to mid crown (Figure 10), which is consistent with previous studies of dwarf mistletoe brooms (Hawksworth and Wiens, 1996).

Concentration of deformities in the low to mid crown can be a common result of intensification processes (Muir and Hennon, 2007; Robinson and Geils, 2006). Increasing average deformity distance to bole with increasing infection severity suggests deformity volume becomes localized at the edges of the crown. Branch growth appears unimpeded by infection likely driving this increase in average distance to bole as seeds continue to infect the thin barked segments near the tips. Branch maximum length may then indicate a maximum distance to bole and an eventual maximum crown width of heavily infected *T. heterophylla*. In heavily infected trees, interior crowns may be mostly branch wood and free space, while the outer shell of the crown is comprised of deformities and effected foliage. This increase in deformity distance from bole also has implications because water path length increases and water transport efficiency of infected branches decreases (Meinzer et al., 2004).

Estimates of crown volume and biomass are often desired for old trees for carbon accounting and growth modeling as carbon allocation shifts once trees reach old growth stages (Ishii et al., 2017; Kramer et al., 2018; Sillett et al., 2010), or for modeling the development of canopies and how this may relate to the spread of dwarf mistletoe (Robinson and Geils, 2006; Swanson et al., 2006; Van Pelt and Nadkarni, 2004).

Allometric models have been produced for young *T. heterophylla*, or uninfected trees in mature and old growth forests, however ours are the first attempt to cover a gradient of dwarf mistletoe infection severity. Further research that expands the sample size and integrates destructive sampling, branch age, and time since infection, with ground-based measurements for predictors could produce more precise models forest managers can use to predict future trajectories of *T. heterophylla* forests infected with *A. tsugense*.

Deformity Class

Arceuthobium tsugense caused-deformities in *T. heterophylla* crowns, took the shape of four distinct classes, depending on where infection occurred on the branch (Figure 5, Table 8). Infections occurring on top of a branch resulted in a spray of foliage perpendicular to the tree (platform); those infecting the main stem of a lateral branch formed a classic witches' broom (classic); those that infected branchlets of primary branches, formed pendulum-shaped deformities that caused the branchlets to droop and foliage to spray out, perpendicularly to the branchlet (pendulous); infections occurring in small branchlets created spindle-shaped swellings commonly associated with early stages of infection (spindle). The classic deformity was the most observed class of deformities larger than 4 cm in one dimension and it is likely that pendulous infections transition into classic deformities with age (Table 8). Deformities smaller than 4 cm in one dimension were not classified, but the vast majority resembled a spindle-shaped swelling, as was expected (Muir and Hennon, 2007).

Hawksworth (1961) described three broom growth forms typical of nonsystemic dwarf mistletoes, using *A. vaginatum* as a model, determined by distance from the bole: typical, volunteer leader, and weeping, with illustrations in Geils et al. (2002). The typical resembles the classic brooms we found in our trees. The volunteer leader broom is characterized as an infected branch that produces branches that grow erect and upright. Weeping brooms exhibit the opposite trait after infection: branchlets droop and hang down below the infected branch at the point of infection. Except for the similarity between our classic broom and the typical broom, these three classes did not apply well to the deformities we observed in our trees. Hawksworth and Wiens (1996) point out secondary infections, where a second infection occurs within an already infected branch or deformity, is rarely observed for the *T. heterophylla – A. tsugense* pathosystems. However, we frequently observed multiple infections within a single deformity, especially large classic brooms. Often, branchlets distal to a deformity would grow towards the edges of the crown and a second infection, causing a small spindle, could be observed there.

The impacts of deformity abundance (as opposed to infection severity or incidence) and class on tree physiology and growth have not been explored in *T. heterophylla*, but previous studies on infected *Pinus jefferyi* and *P. ponderosa* in valuable recreation forests found deformity removal increased host vigor and extended life span (Lightle and Hawksworth, 1973; Scharpf et al., 1987). Stanton (2006) examined radial growth impacts from broom abundance in *P. ponderosa* and found that infection severity explained the majority of growth reductions in their model and that in oldest stand with

the largest trees, deformity abundance appeared to have little to no impact. The impact of deformity abundance on *T. heterophylla* may be more significant than on dry-side *Pinus* spp. as tree growing conditions are more favorable (Waring and Franklin, 1979) and host vigor is associated with dwarf mistletoe vigor (Shaw et al., 2005).

Further modeling is needed to determine if these classes have implications for crown function, spread and intensification, physiological functioning, and if infection classes can be predicted based on location within the crown. These determinations could also help future attempts to assess infection impacts in the crowns of infected *T. heterophylla*, either from the ground or within the tree. Small units of measurement, called "foliar units", are often employed in crown mapping that allow a researcher to quantify leaves, bark, cambium, and wood on complex branches, based on previous destructive sampling, that is not time intensive (Van Pelt and Sillett, 2008). Despite the gaps in knowledge, deformity class may be able to serve a similar role. Classifying deformities was not time intensive and deformities are known to influence host growth, survival, and vigor (Lightle and Hawksworth, 1973; Scharpf et al., 1987), although inclusion of this classification system into other surveys would require a preliminary destructive sampling effort.

Sapwood

While the crown showed evidence for profound change to structure, we found almost no evidence of an effect or relationship between sapwood area, either at *f*-diameter or at base of the live crown, and our measures of infection severity (Figure 12). Meinzer

et al. (2004) measured sapwood area in severely infected and uninfected *T. heterophylla* and found insignificant differences in sapwood area, suggesting alterations to leaf area over carbon allocation were more advantageous. It has been shown that sapwood area is tightly correlated to the live foliage area above it, especially when measured at the base of the live crown (Ishii et al., 2017; Shinozaki et al., 1964b; Waring et al., 1982). Lacking direct measures of leaf area or mass, we substituted the total number of live branches and found a stronger correlation to relative sapwood area at *f*-diameter and at base of the live crown and estimated an increase in relative area as total live branches increased (Figure 12).

These results suggest, it may be beneficial to *A. tsugense* to keep infected branches alive and continue drawing resources from the host, potentially explaining the weak evidence for infection severity's relationship to decreasing live branches and its non-effect on sapwood area. Keeping infected branches alive with ~ 13% less foliage and significantly reduced photosynthetic capacity, would mean carbon accumulation would be severely limited, resulting in adjustments to allocation. Logan et al. (2013) suggested *A. pusillum* infected *Picea glauca* dedicate a disproportionate amount of photoassimilate to branches with low water use efficiency, reflected in severely decreased bole diameter growth while significant reductions to bole diameter growth have been demonstrated in infected *T. heterophylla* (Bell et al., 2020; Marias et al., 2014; Shaw et al., 2008).

Shifts in Crown Form, Implications for Tree Function

The changes in crown structure imply a shift in function, from biomass production and growth, to survival. Some studies have reported initial infections are associated with increases in bole diameter growth potentially due to deformity-caused increases in branch foliage, or that more vigorous trees are more likely to be infected and are growing more rapidly despite infection (Marias et al., 2014; Shaw et al., 2005). Ultimately, infections result in large reductions in height and bole diameter growth as infection severity increases (Bell et al., 2020; Marias et al., 2014; Muir and Hennon, 2007). Top-kill has also been attributed to severe *A. tsugense* infection (Muir and Hennon, 2007). These impacts and other reported in this study drastically change crown structure and physiological function, but the mortality process is still a very slow decline rather than immediate and cause of death cannot always be attributed to dwarf mistletoe, rather increasing susceptibility to other biotic and abiotic mortality agents (Muir and Hennon, 2007).

Arceuthobium tsugense may be driving diversions of photoassimilate from growth related processes to maintenance of infected branches and its own maintenance and reproductive needs (Logan et al., 2013). This further suggests some branches may be net water and nutrient sinks rather than sources. The reduction of photoassimilate available to infected trees for biomass accumulation may be a mechanism to explain previously reported reductions to bole diameter growth (Bell et al., 2020; Marias et al., 2014). Intensification is also shrinking the crown volume further suggesting growth inhibition.

Compensation for alterations in water conductance at the leaf level, have been observed in pruned loblolly pines such that leaf-specific water conductance is maintained (Pataki et al., 1998). Meinzer et al. (2004) reported reductions to overall tree water use for heavily infected *T. heterophylla*, which appeared to be compensated for by reductions to branch foliage and live branches, resulting in maintenance of leaf-specific. Our findings support the reduction to branch foliage, but not the reduction of live branches, suggesting reducing foliage is the preferred mechanism for compensation. Additionally, stem sapwood area remained unaffected by infection severity suggesting conductive tissues may not be altered to maintain water conductance. Remaining branch foliage is increasingly found distal to an infection likely compounding reduced photosynthetic capability and reduced water use efficiency (Marias et al., 2014; Meinzer et al., 2004). Simultaneously, infection intensification results in branches of infected trees supporting 1 to 70 individual infections. When this process is scaled to the whole tree however, we see that these shifts in form and function are due to an exceptionally small amount of deformed tissue. For example, in tree 7, where we observed the highest incidence by far, total deformity volume only reached a maximum of ~ 76 m^3, representing a mere 9% of total crown volume and yet almost all the live foliage was found distal to an infection (Figure 13). Most of the crown volume of trees is likely comprised of woody tissues or space, and minimally, actively photosynthesizing tissues. Therefore, the modest increase in the proportion of crown volume comprised of deformities seems small compared to the total volume, but likely represents almost all of the physiologically relevant tissues in the most severely infected trees.

The outsized impact of *A. tsugense*, relative to the size of its host is phenomenal, especially when compared with the large leafy mistletoes in Loranthaceae. *Arceuthobium tsugense* plants grow to 7 cm in height on average and the plant itself is completely inconspicuous without careful observation of deformities high in the crowns of *T. tsugense* or one of its occasional hosts (Hawksworth and Wiens, 1996). The leaves of the plant are quite reduced and are thought to perform only minor photosynthesis (Hawksworth and Wiens, 1996). However, one infection can produce large deformations in branch form and severely impact growth (Marias et al., 2014; Meinzer et al., 2004). In contrast, species of mistletoe in the *Amyema* genus, are much larger, producing robust, shrub-like plants that are on average 0.5 to 1 m in overall diameter (Shaw et al., 2004). Additionally, the mistletoe leaves in Australia are an important food and water source for birds and mammals (Shaw et al., 2004; Watson, 2001). *Amyema* spp. produce similar impacts to tree form, namely broom-like deformities and branch mortality, but the degree of impact to tree form or growth is minimal compared to *A. tsugense* infections (Shaw et al., 2004).

Incidence and Severity Model Performance

This study was the first to provide a complete survey of all infections within a tree crown of an infected old-growth *T. heterophylla*. However, the incidence of *A. tsugense* infection did not adequately explain the impacts to crown architecture in our study when used alone in a model with a sample across a range of infection severity. Incidence may need to be qualified with a measure of severity, as a high concentration of infections on

one branch would not have the same magnitude of physiological influence on water use dynamics as the same number of infections spread among many live branches (Meinzer et al., 2004). Comparisons of two *T. heterophylla* with the same or similar severity ratings could benefit from inclusion of incidence in models when considering impacts of intensification, such as our trees 7 and 12, both with branch severity measured at 100%. We observed an incidence of 3615 infections in tree 7 and 813 in 12; this enormous difference in incidence likely results in very different influences on tree crown architecture. Stand- and tree-level characteristics common in forest modeling such as density, tree age and size, or tree vigor may also improve incidence model results (Geils et al., 2002; Muir et al., 2004). Attempts to model the epidemiology of *A. tsugense* could benefit from knowledge of incidence within the crown (Robinson and Geils, 2006), where location of female plants is crucial for determining spread within a tree or forest stand. Incidence is likely to be valuable for these applications of infection severity evaluation, but further investigation is required.

Discrepancies in model estimates and R^2 values, when using branch or foliage severity, suggests the effects of *A. tsugense* may be better evaluated using one or the other of these severity measurements. In some cases, foliage severity may be more accurate estimating impacts such as average branch foliage or crown volume. In others, either measure may be inconsequential such as sapwood area, average branch deformity volume, or branch diameters and lengths. These differences likely highlight how infection impacts to crown form are manifested by the tree. For example, we found increasing infection severity to be associated with a decrease in branch foliage, and that

the model with foliage severity as the explanatory variable had the highest R^2. So increasingly affected *T. heterophylla* foliage by *A. tsugense* is likely to drive the reduction in average branch foliage cover, and not simply an increase in the number of infected branches. Future research that incorporates a larger sample size and includes the branch age and estimate of infection date, branch severity, foliage severity, and environmental explanatory variables in a model may further elucidate the degree to which infection severity transforms the crown of an infected *T. heterophylla*, thereby its physiology and further impacts to Northwest forests.

Conclusions

The focus on a comprehensive description of *T. heterophylla* crown architecture through a fine-scale gradient of infection severity by *A. tsugense* utilizing tree climbing is novel in this field and has allowed new insight into the dwarf mistletoe – western hemlock pathosystems. Results from this study suggest that shifts in crown structure imply a shift in function, from biomass production and growth to tree and branch survival. Further implementation of the crown mapping technique as employed in this study, has the potential to add significant clarity to the large, existing body of literature (Muir and Hennon, 2007). Utilizing a fine-scale, infection severity measure can be prohibitively difficult in large, old trees without accessing the crown or felling and compromising data. Previous research has often used the Hawksworth 6-class dwarf mistletoe rating (1977), dividing crowns into infection severity class, which may overlook subtle transformations of the crown.

CHAPTER 3 – GENERAL CONCLUSIONS

Our results suggest shifts in crown structure reflect a shift in function, from biomass production and growth to tree and branch survival. Our models relating increasing dwarf mistletoe infection severity to branch and deformity level response variables exhibited the largest degrees of correlation (Table 6, 7). Little evidence was found for infection severity's correlation with our whole crown and sapwood related variables (Appendix C). Models that lack evidence of correlation however, still provided valuable insights about what may be impacted by increasing severity.

The most notable findings from our branch level modeling was the compelling evidence for a decrease in average branch foliage cover with increasing infection severity (Figure 6). This agrees with previous observations about alterations to hydraulic architecture in by *A. tsugense* to *T. tsugense* (Hawksworth and Wiens, 1996; Meinzer et al., 2004), but contrasts with previous findings in other tree species infected with dwarf mistletoe (Godfree et al., 2003; Sala et al., 2001). The estimated decrease in live branches, increase in dead branches, and a reduction in the proportion of live branches with increasing infection severity showed weak evidence for an association with increasing infection severity (Figure 6). However, decreases in the number of live branches had been previously hypothesized to be a mechanism for infected trees to compensate for infection (Meinzer et al., 2004). The combination of a reduction in average branch foliage cover, residual foliage photosynthetic capacity, and the number of live branches may explain the previous reports of the significant reductions to bole diameter growth (Bell et al., 2020; Marias et al., 2014).

Infection severity showed little evidence for an effect on absolute and relative sapwood area despite reductions to foliage and potential impacts to the number of live branches. Live foliage area or mass has been shown to be linked to the sapwood area of a tree (Shinozaki et al., 1964b; Waring et al., 1982). Meinzer et al. (2004) suggest that it may be more advantageous for the tree to compensate for increased water stress through reductions in foliage than through reductions to water conducting tissue and that the leaves may experience transient changes to their function to maintain water homeostasis.

The lack of expected effect on branch diameter and length contrasts with previous work on *T. heterophylla* branches infected with *A. tsugense*, which found branch diameters increased as a result of infection (Smith, 1969). We did find an association with infection severity and decreasing branch slope 2 angles, defined as the angle between the point at which the branch protrudes from the tree and the tip of the branch. This resulted in decreases to crown volume and suggests an overall compaction of the crown. However, this may not be a result of the same infection process that produces the deformities. Rather severely infected branches that support many deformities may be weighed down. Large deformities are reported to weigh hundreds of kilograms (Muir and Hennon, 2007) and compression wood has been found to be concentrated in tree boles closest to deformed branches (Wellwood, 1956).

Modeling deformity related responses produced our model set with the highest R^2 values. Aside from increasing average distance to bole, we also found evidence for an increase in total deformity volume, proportion of crown in deformity, and the median dwarf mistletoe infection per branch. It has been noted that secondary infections in *T.*

heterophylla are rarely observed but infected branches had between 1 and 70 infections (Hawksworth and Wiens, 1996).

Four distinct deformity classes were observed within the crowns of infected trees. Of the deformities large enough to measure (> 4 cm in length, width, or depth), the classic deformity class was most observed (Table 8). However further research is needed to determine if these classes can be predicted based on location within the crown and of there are differing physiological impacts to infected trees.

Overall crown volume was found to decrease as infection severity increased (Figure 9). Decreasing branch slope 2 angles and decreasing crown depth both contributed to decreasing crown volume, where crowns became less wide and the length of the crowns shortened. As crown volume decreased, the proportion of crown volume comprised of deformation increased. Because the average distance of deformities to bole increased, we observed the increasing deformity volume, shift to the exteriors of the crown and allocation appeared to be localized to the low and mid crowns (Figure 10). Finally, as infection severity increased, foliage became increasingly located distal to infections (Table 5, Foliage Severity; Figure 13). In *Pinus contorta* subsp. *murrayana* stands with dwarf mistletoe infection, Agne et al. (2014) found strong evidence for a decrease in crown volume as infection severity increased and Godfree et al. (2002) showed changes to individual crown structure that led to reduced crown volumes.

In most models, incidence poorly explained variance of the response variable or did not meet model assumptions. The number of individual infections may not be useful in a model alone or at all when examining impacts to tree crowns on a gradient of

infection severity. Models that examine trees already completely infected (branch severity = 100%) could benefit from the inclusion of incidence in a model as differences in the physiology or crown architecture could not be explained by measures of severity. Additionally, any model attempting to assess impacts may need to include stand and tree level characteristics, such as density, tree age and size, or tree vigor (Geils et al., 2002; Muir et al., 2004). Aside from model performance, this also suggests that increasing infection abundance may not create additional draws on host resources, despite the substantial increase in the number of infections per branch as severity increases.

Understanding how *A. tsugense* transforms an infected crown is imperative for predicting how forests act during fire events (Shaw and Agne, 2017), for forest managers meeting certain ecosystem function goals through forest structure (Franklin et al., 2002), and for carbon accounting when *A. tsugense* is appreciably present in a forest (Ishii et al., 2017; Marias et al., 2014). Forest structure has been linked to its ecosystem functions such as benefiting animal biodiversity through providing unique habitat structures (Shaw et al., 2004; Watson, 2001). Therefore, efforts to develop resilient forests benefit from knowledge of changing forest structure due to forest pathogens (Agne et al., 2018; Carey and Wilson, 2001; Ishii et al., 2004).

BIBLIOGRAPHY

Agne, M.C., Beedlow, P.A., Shaw, D.C., Woodruff, D.R., Lee, E.H., Cline, S.P., Comeleo, R.L., 2018. Interactions of predominant insects and diseases with climate change in Douglas-fir forests of western Oregon and Washington, U.S.A. For. Ecol. Manage. 409, 317–332. https://doi.org/10.1016/j.foreco.2017.11.004

Agne, M.C., Shaw, D.C., Woolley, T.J., Queijeiro-Bolãos, M.E., 2014. Effects of Dwarf Mistletoe on Stand Structure of Lodgepole Pine Forests 21-28 Years Post-Mountain Pine Beetle Epidemic in Central Oregon. PLoS One 9. https://doi.org/10.1371/journal.pone.0107532

Anderson, D.L., Schulwitz, S., May, M., Hill, G., Koomjian, W., McClure, C.J.W., 2020. Can increased training and awareness take forest research to new heights? Trees, For. People 1, 100005. https://doi.org/10.1016/j.tfp.2020.100005

Barton, K., 2019. MuMIn: Multi-Model Inference. R package version 1.43.15. https://CRAN.R-project.org/package=MuMIn

Bell, D.M., Pabst, R.J., Shaw, D.C., 2020. Tree growth declines and mortality were associated with a parasitic plant during warm and dry climatic conditions in a temperate coniferous forest ecosystem. Glob. Chang. Biol. 26, 1714–1724. https://doi.org/10.1111/gcb.14834

Bormann, B.T., 1990. Diameter-based biomass regression models ignore large sapwood-related variation in Sitka spruce. Can. J. For. Res. 20, 1098–1104. https://doi.org/10.1139/x90-145

Carey, A.B., Wilson, S.M., 2001. Induced Spatial Heterogeneity in Forest Canopies: Responses of Small Mammals. J. Wildl. Manage. 65, 1014. https://doi.org/10.2307/3803050

Castello, J.D., Leopold, D.J., Smallidge, P.J., 1995. Pathogens, Patterns, and Processes in Forest Ecosystems. Bioscience 45, 16–24. https://doi.org/10.2307/1312531

Davis, R.J., 2010. Johnson's Hairstreak Surveys in Oregon and Washington.

Dunham, P.A., 2008. Incidence of Insects, Diseases, and Other Damaging Agents in Oregon Forests. Resour. Bull. PNW-RB-257. Portland, OR US Dep. Agric. For. Serv. Pacific Northwest Res. Station. 89 p.

Ewers, F.W., Zimmermann, M.H., 1984. The hydraulic architecture of balsam fir (*Abies balsamea*). Physiol. Plant. 60, 453–458. https://doi.org/10.1111/j.1399-3054.1984.tb04911.x

Fahey, R.T., Alveshere, B.C., Burton, J.I., D'Amato, A.W., Dickinson, Y.L., Keeton, W.S., Kern, C.C., Larson, A.J., Palik, B.J., Puettmann, K.J., Saunders, M.R., Webster, C.R., Atkins, J.W., Gough, C.M., Hardiman, B.S., 2018. Shifting conceptions of complexity in forest management and silviculture. For. Ecol. Manage. 421, 59–71. https://doi.org/10.1016/j.foreco.2018.01.011

Forsman, E.D., Meslow, C.E., Wight, H.M., 1984. Distribution and Ecology of the Spotted Owl in Oregon. Wildl. Monogr. 3–64.

Franklin, J.F., Dyrness, C.T., 1973. Natural Vegetation of Oregon and Washington. Gen. Tech. Rep. PNW-GTR-008. Portland, OR U.S. Dep. Agric. For. Serv. Pacific Northwest Res. Station. 427 p.

Franklin, J.F., Spies, T.A., Pelt, R. Van, Carey, A.B., Thornburgh, D.A., Berg, D.R., Lindenmayer, D.B., Harmon, M.E., Keeton, W.S., Shaw, D.C., Bible, K., Chen, J., 2002. Disturbances and structural development of natural forest ecosystems with silvicultural implications, using Douglas-fir forests as an example. For. Ecol. Manage. 155, 399–423. https://doi.org/10.1016/S0378-1127(01)00575-8

Geils, B.W., Tovar, J.C., Moody, B., 2002. Mistletoes of North American conifers, Gen. Tech. Rep. RMRS–GTR–98. Ogden, UT: U.S. Department of Agriculture, Forest Service, Rocky Mountain Research Station. 123 p. https://doi.org/10.2737/RMRS-GTR-98

Glatzel, G., Geils, B.W., 2009. Mistletoe ecophysiology: Host-parasite interactions. Botany 87, 10–15. https://doi.org/10.1139/B08-096

Godfree, R.C., Tinnin, R.O., Forbes, R.B., 2003. Relationships between dwarf mistletoe and the canopy structure of an old-growth lodgepole pine forest in central Oregon. Can. J. For. Res. 33, 997–1009. https://doi.org/10.1139/x03-024

Godfree, R.C., Tinnin, R.O., Forbes, R.B., 2002. The effects of dwarf mistletoe, witches' brooms, stand structure, and site characteristics on the crown architecture of lodgepole pine in Oregon. Can. J. For. Res. 32, 1360–1371. https://doi.org/10.1139/x02-058

Griebel, A., Watson, D., Pendall, E., 2017. Mistletoe, friend and foe: Synthesizing ecosystem implications of mistletoe infection. Environ. Res. Lett. 12. https://doi.org/10.1088/1748-9326/aa8fff

Hansen, E.M., Goheen, E.M., 2000. *Phellinus weirii* and Other Native Root Pathogens as Determinants of Forest Structure and Process in Western North America. Annu. Rev. Phytopathol. 38, 515–539. https://doi.org/10.1146/annurev.phyto.38.1.515

Hawksworth, F.G., 1977. The 6-class dwarf mistletoe rating system. USDA For. Serv. Gen. Tech. Report, Rocky Mt. For. Range Exp. Station. RM-48.

Hawksworth, F.G., 1961. Dwarf Mistletoe of Ponderosa Pine in the Southwest. USDA For. Serv. Rocky Mt. For. Range Exp. Station. Tech. Bull. No. 1246.

Hawksworth, F.G., Wiens, D., 1996. Dwarf Mistletoes: Biology, Pathology, and Systematics, Agriculture Handbook 709. https://doi.org/ISBN-13: 978-92-95044-73-9

Hoffman, C., Mathiasen, R., Sieg, C.H., 2007. Dwarf mistletoe effects on fuel loadings in ponderosa pine forests in northern Arizona. Can. J. For. Res. 37, 662–670. https://doi.org/10.1139/X06-259

Ishii, H.R., Sillett, S.C., Carroll, A.L., 2017. Crown dynamics and wood production of Douglas-fir trees in an old-growth forest. For. Ecol. Manage. 384, 157–168. https://doi.org/10.1016/j.foreco.2016.10.047

Ishii, H.T., Tanabe, S., Hiura, T., 2004. Exploring the relationships among canopy structure, stand productivity, and biodiversity of temperate forest ecosystems. For. Sci. 50, 342–355. https://doi.org/10.1093/forestscience/50.3.342

Jepson, J., 2000. The tree climber's companion: a reference and training manual for professional tree climbers. Beaver Tree Pub. https://doi.org/0615112900

Kramer, R.D., Sillett, S.C., Van Pelt, R., 2018. Quantifying aboveground components of *Picea sitchensis* for allometric comparisons among tall conifers in North American rainforests. For. Ecol. Manage. 430, 59–77. https://doi.org/10.1016/j.foreco.2018.07.039

Lightle, P.C., Hawksworth, F.G., 1973. Control of dwarf mistletoe in a heavily used ponderosa pine recreation forest : Grand Canyon, Arizona. USDA Forest Service, Research Paper, Rocky Mountain Forest Range Experimental Station, RM-106.

Logan, B.A., Reblin, J.S., Zonana, D.M., Dunlavey, R.F., Hricko, C.R., Hall, A.W., Schmiege, S.C., Butschek, R.A., Duran, K.L., Emery, R.J.N., Kurepin, L. V., Lewis, J.D., Pharis, R.P., Phillips, N.G., Tissue, D.T., 2013. Impact of eastern dwarf mistletoe (*Arceuthobium pusillum*) on host white spruce (*Picea glauca*) development, growth and performance across multiple scales. Physiol. Plant. 147, 502–513. https://doi.org/10.1111/j.1399-3054.2012.01681.x

Lutz, J.A., Furniss, T.J., Johnson, D.J., Davies, S.J., Allen, D., Alonso, A., Anderson-Teixeira, K.J., Andrade, A., Baltzer, J., Becker, K.M.L., Blomdahl, E.M., Bourg, N.A., Bunyavejchewin, S., Burslem, D.F.R.P., Cansler, C.A., Cao, K., Cao, M.,

Cárdenas, D., Chang, L.W., Chao, K.J., Chao, W.C., Chiang, J.M., Chu, C., Chuyong, G.B., Clay, K., Condit, R., Cordell, S., Dattaraja, H.S., Duque, A., Ewango, C.E.N., Fischer, G.A., Fletcher, C., Freund, J.A., Giardina, C., Germain, S.J., Gilbert, G.S., Hao, Z., Hart, T., Hau, B.C.H., He, F., Hector, A., Howe, R.W., Hsieh, C.F., Hu, Y.H., Hubbell, S.P., Inman-Narahari, F.M., Itoh, A., Janík, D., Kassim, A.R., Kenfack, D., Korte, L., Král, K., Larson, A.J., Li, Y. De, Lin, Y., Liu, S., Lum, S., Ma, K., Makana, J.R., Malhi, Y., McMahon, S.M., McShea, W.J., Memiaghe, H.R., Mi, X., Morecroft, M., Musili, P.M., Myers, J.A., Novotny, V., de Oliveira, A., Ong, P., Orwig, D.A., Ostertag, R., Parker, G.G., Patankar, R., Phillips, R.P., Reynolds, G., Sack, L., Song, G.Z.M., Su, S.H., Sukumar, R., Sun, I.F., Suresh, H.S., Swanson, M.E., Tan, S., Thomas, D.W., Thompson, J., Uriarte, M., Valencia, R., Vicentini, A., Vrška, T., Wang, X., Weiblen, G.D., Wolf, A., Wu, S.H., Xu, H., Yamakura, T., Yap, S., Zimmerman, J.K., 2018. Global importance of large-diameter trees. Glob. Ecol. Biogeogr. 27, 849–864. https://doi.org/10.1111/geb.12747

Marias, D.E., Meinzer, F.C., Woodruff, D.R., Shaw, D.C., Voelker, S.L., Brooks, J.R., Lachenbruch, B., Falk, K., McKay, J., 2014. Impacts of dwarf mistletoe on the physiology of host *Tsuga heterophylla* trees as recorded in tree-ring C and O stable isotopes. Tree Physiol. 34, 595–607. https://doi.org/10.1093/treephys/tpu046

Mathiasen, R.L., Nickrent, D.L., Shaw, D.C., Watson, D.M., 2008. Mistletoes: Pathology, Systematics, Ecology, and Management. Plant Dis. 92, 988–1006.

Meinzer, F.C., Woodruff, D.R., Shaw, D.C., 2004. Integrated responses of hydraulic architecture, water and carbon relations of western hemlock to dwarf mistletoe infection. Plant, Cell Environ. 27, 937–946. https://doi.org/10.1111/j.1365-3040.2004.01199.x

Michel, A.K., Winter, S., 2009. Tree microhabitat structures as indicators of biodiversity in Douglas-fir forests of different stand ages and management histories in the Pacific Northwest, U.S.A. For. Ecol. Manage. 257, 1453–1464. https://doi.org/10.1016/j.foreco.2008.11.027

Muir, J.A., Hennon, P.E., 2007. A synthesis of the literature on the biology, ecology, and management of Western Hemlock dwarf mistletoe. USDA For. Serv. - Gen. Tech. Rep. PNW-GTR 1–142. https://doi.org/10.2737/PNW-GTR-718

Muir, J.A., Robinson, D.C.E., Geils, B.W., 2004. Characterizing the effects of dwarf mistletoe and other diseases for sustainable forest management. BC J. Ecosyst. Manag. 3.

Nakagawa, S., Johnson, P.C.D., Schielzeth, H., 2017. The coefficient of determination R2 and intra-class correlation coefficient from generalized linear mixed-effects models revisited and expanded. J. R. Soc. Interface 14. https://doi.org/10.1098/rsif.2017.0213

Nakagawa, S., Schielzeth, H., 2013. A general and simple method for obtaining R2 from generalized linear mixed-effects models. Methods Ecol. Evol. 4, 133–142. https://doi.org/10.1111/j.2041-210x.2012.00261.x

Parker, G.G., Harmon, M.E., Lefsky, M.A., Chen, J., Van Pelt, R., Weiss, S.B., Thomas, S.C., Winner, W.E., Shaw, D.C., Franklin, J.F., 2004. Three-dimensional structure of an old-growth Pseudotsuga-tsuga canopy and its implications for radiation balance, microclimate, and gas exchange. Ecosystems 7, 440–453. https://doi.org/10.1007/s10021-004-0136-5

Parmeter, J R. Jr., 1978. Forest Stand Dynamics and Ecological Factors in Relation to Dwarf Mistletoe Spread, Impact, and Control, in: Scharpf, R.F., Parmeter, John R. Jr. (Eds.), Symposium on Dwarf Mistletoe Control Through Forest Management. Berkeley, California, pp. 16–30.

Pataki, D.E., Oren, R., Phillips, N., 1998. Responses of sap flux and stomatal conductance of Pinus taeda L. trees to stepwise reductions in leaf area. J. Exp. Bot. 49, 871–878. https://doi.org/10.1093/jxb/49.322.871

R Core Team, 2019. R: A language and environment for statistical computing. R Foundation for Statistical Computing, Vienna, Austria. URL https://www.R-project.org/.

Ramsey, F., Schafer, D., 2012. The statistical sleuth: a course in methods of data analysis. Cengage Learning.

Reilly, M.J., Spies, T.A., 2016. Disturbance, tree mortality, and implications for contemporary regional forest change in the Pacific Northwest. For. Ecol. Manage. 374, 102–110. https://doi.org/10.1016/j.foreco.2016.05.002

Reilly, M.J., Spies, T.A., 2015. Regional variation in stand structure and development in forests of Oregon, Washington, and inland Northern California. Ecosphere 6, 1–27. https://doi.org/10.1890/ES14-00469.1

Robinson, D.C.E., Geils, B.W., 2006. Modelling dwarf mistletoe at three scales: life history, ballistics and contagion. Ecol. Model. https://doi.org/10.1016/j.ecolmodel.2006.06.007

Sala, A., Carey, E. V., Callaway, R.M., 2001. Dwarf mistletoe affects whole-tree water relations of Douglas fir and western larch primarily through changes in leaf to sapwood ratios. Oecologia 126, 42–52. https://doi.org/10.1007/s004420000503

Sattler, D.F., Comeau, P.G., 2016. Crown allometry and application of the pipe model theory to white spruce (*Picea glauca* (Moench) Voss) and aspen (*Populus tremuloides* Michx.) in the western boreal forest of Canada. Can. J. For. Res. 46, 262–273. https://doi.org/10.1139/cjfr-2015-0165

Scharpf, R.F., Smith, R.S., Vogler, D., 1987. Pruning dwarf mistletoe brooms reduces stress on Jeffrey pines, Cleveland National Forest, California. USDA For. Serv. Res. Pap. Pacific Southwest For. Range Exp. Station. PSW-186.

Sellin, A., Kupper, P., 2006. Spatial variation in sapwood area to leaf area ratio and specific leaf area within a crown of silver birch. Trees 20, 311–319. https://doi.org/10.1007/s00468-005-0042-2

Shaw, D., Freeman, E.A., Mathiasen, R.L., 2000. Evaluating the Accuracy of Ground-Based Hemlock Dwarf Mistletoe Rating: A Case Study Using the Wind River Canopy Crane. West. J. Appl. For. 15, 8–14. https://doi.org/10.1093/wjaf/15.1.8

Shaw, D., Greene, S., 2003. Wind River Canopy Crane Research Facility and Wind River Experimental Forest. Bull. Ecol. Soc. Am. 84, 115–121. https://doi.org/10.1890/0012-9623(2003)84[115:wrccrf]2.0.co;2

Shaw, D.C., Agne, M.C., 2017. Fire and dwarf mistletoe (Viscaceae: *Arceuthobium* species) in western north America: Contrasting *Arceuthobium tsugense* and *Arceuthobium americanum*. Botany 95, 231–246. https://doi.org/10.1139/cjb-2016-0245

Shaw, D.C., Chen, J., Freeman, E.A., Braun, D.M., 2005. Spatial and population characteristics of dwarf mistletoe infected trees in an old-growth Douglas-fir - western hemlock forest. Can. J. For. Res. 35, 990–1001. https://doi.org/10.1139/x05-022

Shaw, D.C., Edmonds, R.L., Littke, W.R., Browning, J.E., Russel, K.W., 1995. Incidence of wetwood and decay in precommercially thinned western hemlock stands. Can. J. For. Res. 25, 1269–1277. https://doi.org/https://doi.org/10.1139/x95-140

Shaw, D.C., Huso, M., Bruner, H., 2008. Basal area growth impacts of dwarf mistletoe on western hemlock in an old-growth forest. Can. J. For. Res. 38, 576–583. https://doi.org/10.1139/X07-174Shaw, D.C., Mathiasen, R.L., 2013. Forest diseases caused by higher parasitic plants: Mistletoes, in: Infectious Forest

Diseases. CABI Publishing, pp. 97–114. https://doi.org/10.1079/9781780640402.0097

Shaw, D.C., Mathiasen, R.L., 2013. Forest diseases caused by higher parasitic plants: Mistletoes, in: Infectious Forest Diseases. CABI Publishing, pp. 97–114. https://doi.org/10.1079/9781780640402.0097

Shaw, D.C., Watson, D.M., Mathiasen, R.L., 2004. Comparison of dwarf mistletoes (*Arceuthobium* spp., Viscaceae) in the western United States with mistletoes (*Amyema* spp., Loranthaceae) in Australia - Ecological analogs and reciprocal models for ecosystem management. Aust. J. Bot. 52, 481–498. https://doi.org/10.1071/BT03074

Shaw, D.C., Weiss, S.B., 2000. Canopy Light and the Distribution of Hemlock Dwarf Mistletoe (*Arceuthobium tsugense* [Rosendahl] G.N. Jones subsp. *tsugense*) Aerial Shoots in an Old-growth Douglas-fir/Western Hemlock Forest. Northwest Sci. 74, 306–315.

Shinozaki, K., Yoda, K., Hozumi, K., Kira, T., 1964a. A Quantitative Analysis of Plant Form-the Pipe Model Theory : I. Basic Analyses. Japanese J. Ecol. 14, 97–105. https://doi.org/10.18960/seitai.14.3_97

Shinozaki, K., Yoda, K., Hozumi, K., Kira, T., 1964b. A Quantitative Analysis of Plant Form-the Pipe Model Theory : II. Further Evidence of the Theory and Its Application in Forest Ecology. Japanese J. Ecol. 14, 133–139. https://doi.org/10.18960/seitai.14.4_133

Sillett, S.C., Van Pelt, R., Carroll, A.L., Campbell-Spickler, J., Coonen, E.J., Iberle, B., 2019. Allometric equations for *Sequoia sempervirens* in forests of different ages. For. Ecol. Manage. 433, 349–363. https://doi.org/10.1016/j.foreco.2018.11.016

Sillett, S.C., Van Pelt, R., Freund, J.A., Campbell-Spickler, J., Carroll, A.L., Kramer, R.D., 2018. Development and dominance of Douglas-fir in North American rainforests. For. Ecol. Manage. 429, 93–114. https://doi.org/10.1016/j.foreco.2018.07.006

Sillett, S.C., Van Pelt, R., Koch, G.W., Ambrose, A.R., Carroll, A.L., Antoine, M.E., Mifsud, B.M., 2010. Increasing wood production through old age in tall trees. For. Ecol. Manage. 259, 976–994. https://doi.org/10.1016/j.foreco.2009.12.003

Smith, R., 1969. Assessing Dwarf Mistletoe on Western Hemlock. For. Sci. 15, 277–285. https://doi.org/10.1093/forestscience/15.3.277

Smith, W.K., Brewer, C.A., 1994. The Adaptive Importance of Shoot and Crown Architecture in Conifer Trees. Am. Nat. 143, 528–532.

Spies, T.A., 2016. LiDAR data (October 2011) for the Upper Blue River Watershed, Willamette National Forest. Long-Term Ecological Research. Forest Science Data Bank, Corvallis, OR. [Database]. Available: http://andlter.forestry.oregonstate.edu/data/abstract.aspx?dbcode=GI011. https://doi.org/10.6073/pasta/8e4f57bafaaad5677977dee51bb3077c. Accessed 2020-07-28.

Spies, T.A., Duncan, S.L., 2012. Old growth in a new world: a Pacific Northwest icon reexamined. Island Press.

Spies, T.A., Franklin, J.F., 1991. The Structure of Natural Young, Mature, and Old-Growth Douglas-fir Forests in Oregon and Washington. USDA For. Serv. Gen. Tech. Rep. PNW-GTR-285. https://doi.org/10.1111/1750-3841.12978

Spies, T.A., Stine, P.A., Gravenmier, R., Long, J.W., Reilly, M.J., 2018. Synthesis of Science to Inform Land Management Within the Northwest Forest Plan Area. Gen. Tech. Rep. PNW-GTR_966 1, 1020.

Stanton, S., 2006. The differential effects of dwarf mistletoe infection and broom abundance on the radial growth of managed ponderosa pine. For. Ecol. Manage. 223, 318–326. https://doi.org/10.1016/j.foreco.2005.11.011

Stephenson, N.L., Das, A.J., Condit, R., Russo, S.E., Baker, P.J., Beckman, N.G., Coomes, D.A., Lines, E.R., Morris, W.K., Rüger, N., Álvarez, E., Blundo, C., Bunyavejchewin, S., Chuyong, G., Davies, S.J., Duque, Á., Ewango, C.N., Flores, O., Franklin, J.F., Grau, H.R., Hao, Z., Harmon, M.E., Hubbell, S.P., Kenfack, D., Lin, Y., Makana, J.R., Malizia, A., Malizia, L.R., Pabst, R.J., Pongpattananurak, N., Su, S.H., Sun, I.F., Tan, S., Thomas, D., Van Mantgem, P.J., Wang, X., Wiser, S.K., Zavala, M.A., 2014. Rate of tree carbon accumulation increases continuously with tree size. Nature 507, 90–93. https://doi.org/10.1038/nature12914

Swanson, F.J., Jones, J.A., 2002. Geomorphology and hydrology of the HJ Andrews experimental forest, Blue River, Oregon. F. Guid. to Geol. Process. Cascadia, Oregon Dep. Geol. Minderal Ind. Spec. Pap. 36 289–313.

Swanson, M.E., Shaw, D.C., Marosi, T.K., 2006. Distribution of western hemlock dwarf mistletoe (*Arceuthobium tsugense* [Rosendahl] G.N. Jones subsp. *tsugense*) in mature and old-growth Douglas-fir (*Pseudotsuga menziesii* [Mirb.] Franco) forests. Northwest Sci. 80, 207–217.

Tepley, A.J., Swanson, F.J., Spies, T.A., 2013. Fire-mediated pathways of stand development in Douglas-fir/western hemlock forests of the Pacific Northwest, USA. Ecology 94, 1729–1743. https://doi.org/10.1890/12-1506.1

Trummer, L.M., Hennon, P.E., Hansen, E.M., Muir, P.S., 1998. Modeling the incidence and severity of hemlock dwarf mistletoe in 110-year-old wind-disturbed forests in Southeast Alaska. Can. J. For. Res. 28, 1501–1508. https://doi.org/10.1017/CBO9781107415324.004

Van Pelt, R., Nadkarni, N.M., 2004. Development of canopy structure in *Pseudotsuga menziesii* forests in the southern Washington Cascades. For. Sci. 50, 326–341. https://doi.org/10.1093/forestscience/50.3.326

Van Pelt, R., North, M.P., 1999. Testing a ground-based canopy model using the Wind River Canopy Crane. Selbyana 20, 357–362.

Van Pelt, R., Sillett, S.C., 2008. Crown development of coastal *Pseudotsuga menziesii*, including a conceptual model for tall conifers. Ecol. Monogr. 78, 283–311. https://doi.org/10.1890/07-0158.1

Van Pelt, R., Sillett, S.C., Nadkarni, N.M., 2004. Quantifying and Visualizing Canopy Structure in Tall Forests. Methods and a Case Study., in: Lowman, M.D., Rinker, H.B. (Eds.), Forest Canopies: Second Edition. Elsevier Academic Press, New York, pp. 49–72. https://doi.org/10.1016/B978-012457553-0/50007-1

Venables, W.N., Ripley, B.D., 2002. Modern Applied Statistics with S, Fourth. ed. Springer, New York. ISBN 0-387-95457-0

Waring, R.H., Franklin, J.F., 1979. Evergreen Coniferous Forests of the Pacific Northwest. Am. Assoc. Adv. Sci. 204, 1380–1386. https://doi.org/10.1126/science.204.4400.1380

Waring, R.H., Schroeder, P.E., Oren, R., 1982. Application of the pipe model theory to predict canopy leaf area. Can. J. For. Res. 12, 556–560. https://doi.org/10.1139/x82-086

Watson, D.M., 2001. Mistletoe - A keystone resource in forests and woodlands worldwide. Annu. Rev. Ecol. Syst. 32, 219–249. https://doi.org/10.1146/annurev.ecolsys.32.081501.114024

Wellwood, R.W., 1956. Some Effects of Dwarf Mistletoe on Western Hemlock. For. Chron. 32, 282–296. https://doi.org/10.5558/tfc32282-3

Winter, L.E., Brubaker, L.B., Franklin, J.F., Miller, E.A., DeWitt, D.Q., 2002. Canopy disturbances over the five-century lifetime of an old-growth Douglas-fir stand in the Pacific Northwest. Can. J. For. Res. 32, 1057–1070. https://doi.org/10.1139/x02-030

Zald, H.S.J., Spies, T.A., Seidl, R., Pabst, R.J., Olsen, K.A., Steel, E.A., 2016. Complex mountain terrain and disturbance history drive variation in forest aboveground live carbon density in the western Oregon Cascades, USA. For. Ecol. Manage. 366, 193–207. https://doi.org/10.1016/j.foreco.2016.01.036

APPENDICES

A. Full set of model results for the branch-related response variables.

The estimated slope, 95% confidence intervals, test statistics and R^2 for each fixed effect and response variable. Coefficient estimates represent a shift from 0 to 100% for branch and foliage severity and a shift from 0 to 100 infections for incidence.

Response	Model Type	Fixed Effect	Coefficient Estimate	Low 95% CI	High 95% CI	F	df	χ^2	p	R^2
Average Branch Diameter	LM	Branch Severity	0.05	-1.08	1.17	0.01	1, 14	---	0.931	0.00
		Foliage Severity	-0.02	-1.13	1.09	0.00	1, 14	---	0.969	0.00
		Incidence	0.00	0.00	0.00	0.10	1, 14	---	0.757	0.01
Median Branch Diameter	LM	Branch Severity	0.02	-1.03	1.07	0.00	1, 14	---	0.967	0.00
		Foliage Severity	0.02	-1.01	1.05	0.00	1, 14	---	0.971	0.00
		Incidence	0.01	-0.03	0.05	0.29	1, 14	---	0.599	0.02
Max Branch Diameter	LM	Branch Severity	0.60	-2.64	3.84	0.16	1, 14	---	0.697	0.01
		Foliage Severity	0.29	-2.90	3.49	0.04	1, 14	---	0.847	0.00
		Incidence	0.00	-0.14	0.14	0.00	1, 14	---	0.960	0.00
Average Branch Length	LM	Branch Severity	-0.33	-1.08	0.43	0.86	1, 14	---	0.370	0.06
		Foliage Severity	-0.30	-1.05	0.44	0.76	1, 14	---	0.397	0.05

		Incidence	0.01	0.00	0.00	0.65	1, 14	---	0.432	0.04
Median Branch Length	LM	Branch Severity	-0.39	-1.14	0.36	1.26	1, 14	---	0.280	0.08
		Foliage Severity	-0.36	-1.10	0.38	1.25	1, 14	---	0.311	0.07
		Incidence	0.00	-0.02	0.04	0.32	1, 14	---	0.582	0.02
Max Branch Length	LM	Branch Severity	-0.99	-2.81	0.83	1.35	1, 14	---	0.264	0.09
		Foliage Severity	-0.94	-2.73	0.86	1.25	1, 14	---	0.282	0.08
		Incidence	0.02	-0.06	0.10	0.19	1, 14	---	0.673	0.01
Average Slope 1	LM	Branch Severity	7.02	-0.56	14.61	3.95	1, 14	---	0.067	0.22
		Foliage Severity	4.53	-3.50	12.55	1.46	1, 14	---	0.246	0.09
		Incidence	0.17	-0.19	0.52	1.01	1, 14	---	0.331	0.07
Median Slope 1	LM	Branch Severity	7.04	-0.40	14.48	4.11	1, 14	---	0.062	0.23
		Foliage Severity	5.02	-2.78	12.82	1.90	1, 14	---	0.189	0.12
		Incidence	0.17	-0.18	0.52	1.09	1, 14	---	0.315	0.07
Average Slope 2	LM	Branch Severity	-6.88	-22.77	9.01	0.86	1, 14	---	0.369	0.06
		Foliage Severity	-11.73	-26.33	2.88	2.97	1, 14	---	0.107	0.17
		Incidence	-0.17	-0.86	0.52	0.28	1, 14	---	0.605	0.02
Median Slope 2	LM	Branch Severity	-8.03	-24.88	8.82	1.04	1, 14	---	0.324	0.07
		Foliage Severity	-13.51	-28.81	1.80	3.58	1, 14	---	0.079	0.20
		Incidence	-0.20	-0.94	0.53	0.35	1, 14	---	0.562	0.02

Average Branch Foliage	LM	Branch Severity	-10.96	-18.55	-3.38	9.61	1, 14	---	0.008	0.41
		Foliage Severity	-13.39	-19.27	-7.51	23.82	1, 14	---	0.000	0.63
		Incidence	-0.32	-0.69	0.06	3.17	1, 14	---	0.097	0.18
Number of Live Branches	GLM	Branch Severity	0.76	0.55	1.06	---	1	2.35	0.126	0.14
		Foliage Severity	0.76	0.55	1.06	---	1	2.46	0.117	0.14
		Incidence	1.00	0.99	1.02	---	1	0.01	0.931	0.00
Number of Dead Branches	GLM	Branch Severity	1.36	0.89	2.08	---	1	1.88	0.170	0.11
		Foliage Severity	1.37	0.92	2.04	---	1	2.20	0.138	0.13
		Incidence	1.01	1.00	1.03	---	1	2.48	0.115	0.14
Total Number of Branches	GLM	Branch Severity	0.86	0.67	1.10	---	1	1.43	0.232	0.09
		Foliage Severity	0.87	0.68	1.10	---	1	1.31	0.253	0.08
		Incidence	1.00	0.99	1.01	---	1	0.43	0.512	0.03
Live Proportion	GLM	Branch Severity	0.56	0.29	1.05	3.26	1, 14	---	0.090	0.01
		Foliage Severity	0.55	0.30	1.01	3.74	1, 14	---	0.070	0.01
		Incidence	0.99	0.96	1.01	0.84	1, 14	---	0.380	0.00

B. Full set of model results for the deformity-related response variables.

The estimated slope, 95% confidence intervals, test statistics and R^2 for each fixed effect and response variable. Coefficient estimates represent a shift from 0 to 100% for branch and foliage severity and a shift from 0 to 100 infections for incidence.

Response	Model Type	Fixed Effect	Coefficient Estimate	Low 95% CI	High 95% CI	F	df	χ^2	p	R^2
Average Deformity Distance to Bole	LM	Branch Severity	3.17	1.62	4.70	19.43	1, 14	---	0.001	0.58
		Foliage Severity	2.29	0.36	4.22	6.47	1, 14	---	0.023	0.32
		Incidence	0.11	0.02	0.19	7.81	1, 14	---	0.014	0.36
Average Branch Deformity Volume	LM	Branch Severity	0.09	-0.20	0.37	0.49	1, 14	---	0.501	0.05
		Foliage Severity	0.09	-0.10	0.28	1.21	1, 14	---	0.299	0.12
		Incidence	0.00	0.00	0.00	0.06	1, 14	---	0.808	0.01
Total Deformity Volume	LM	Branch Severity	49.40	22.63	76.17	15.67	1, 14	---	0.001	0.53
		Foliage Severity	55.12	33.54	76.70	30	1, 14	---	0.000	0.68
		Incidence	---	---	---	---	1, 14	---	---	---
Proportion of Crown in Deformity	LM	Branch Severity	0.06	0.02	0.10	10.24	1, 14	---	0.006	0.42
		Foliage Severity	0.07	0.04	0.11	18.85	1, 14	---	0.001	0.57
		Incidence	---	---	---	---	1, 14	---	---	---

Median Dwarf Mistletoe Infection	GLM	Branch Severity	27.20	9.60	90.06	---	1	23.98	0.000	0.78
		Foliage Severity	14.12	5.67	37.85	---	1	17.88	0.000	0.67
		Incidence	1.11	1.05	1.20	---	1	10.89	0.001	0.49

C. Full set of model results for the whole tree and sapwood-related response variables.

The estimated slope, 95% confidence intervals, test statistics and R^2 for each fixed effect and response variable. Coefficient estimates represent a shift from 0 to 100% for branch and foliage severity and a shift from 0 to 100 infections for incidence.

Response	Model Type	Fixed Effect	Coefficient Estimate	Low 95% CI	High 95% CI	F	df	χ^2	p	R^2
Minimum Branch Height	LM	Branch Severity	2.49	-2.60	7.57	1.1	1, 14	---	0.312	0.07
		Foliage Severity	2.44	-2.55	7.44	1.1	1, 14	---	0.312	0.07
		Incidence	-0.02	-0.24	0.21	0.03	1, 14	---	0.873	0.00
Crown Depth	LM	Branch Severity	-6.25	-13.19	0.70	3.72	1, 14	---	0.074	0.21
		Foliage Severity	-5.77	-12.70	1.15	3.19	1, 14	---	0.096	0.19
		Incidence	-0.11	-0.44	0.21	0.55	1, 14	---	0.470	0.04
Frusta-based Crown Volume	LM	Branch Severity	-632.87	-1330.30	64.57	5.46	1, 14	---	0.072	0.21
		Foliage Severity	-696.34	-1357.10	-35.58	7.72	1, 14	---	0.040	0.27
		Incidence	-2.38	-35.40	31.14	0.12	1, 14	---	0.881	0.00
Sapwood Area at f DBH	LM	Branch Severity	-0.04	-0.09	0.02	1.74	1, 14	---	0.208	0.11
		Foliage Severity	-0.03	-0.09	0.03	1.33	1, 14	---	0.269	0.09
		Incidence	0.00	0.00	0.00	0.06	1, 14	---	0.804	0.00

Relative Sapwood Area at f-DBH	LM	Branch Severity	-0.02	-0.24	0.19	0.06	1, 14	---	0.816	0.00
		Foliage Severity	-0.04	-0.25	0.17	0.16	1, 14	---	0.694	0.01
		Incidence	0.00	0.00	0.00	0.02	1, 14	---	0.891	0.00
Sapwood Area at Live Crown Base	LM	Branch Severity	-0.03	-0.08	0.02	1.52	1, 14	---	0.239	0.10
		Foliage Severity	-0.02	-0.07	0.03	1.00	1, 14	---	0.334	0.07
		Incidence	0.00	0.00	0.00	0.02	1, 14	---	0.898	0.00
Relative Sapwood Area at Live Crown Base	LM	Branch Severity	-0.02	-0.19	0.15	0.04	1, 14	---	0.838	0.00
		Foliage Severity	-0.01	-0.18	0.16	0.02	1, 14	---	0.890	0.00
		Incidence	0.00	0.00	0.00	0.04	1, 14	---	0.844	0.00